

UNIVERSITI MALAYSIA PAHANG

BORANG PENGESAHAN STATUS TESIS♦

JUDUL: NUMERICAL INVESTIGATION ON THE EFFECT OF DIFFERENT STRUT ANGLE TO THE CEREBRAL ANEURYSM

SESI PENGAJIAN: 2009/2010

Saya NOOR HARLIANA BINTI A.HAMID (871009-02-5452)
(HURUF BESAR)

mengaku membenarkan tesis (Sarjana Muda/~~Sarjana~~ /~~Doktor Falsafah~~)* ini disimpan di Perpustakaan dengan syarat-syarat kegunaan seperti berikut:

1. Tesis adalah hakmilik Universiti Malaysia Pahang (UMP).
2. Perpustakaan dibenarkan membuat salinan untuk tujuan pengajian sahaja.
3. Perpustakaan dibenarkan membuat salinan tesis ini sebagai bahan pertukaran antara institusi pengajian tinggi.
4. **Sila tandakan (√)

SULIT

(Mengandungi maklumat yang berdarjah keselamatan atau kepentingan Malaysia seperti yang termaktub di dalam AKTA RAHSIA RASMI 1972)

TERHAD

(Mengandungi maklumat TERHAD yang telah ditentukan oleh organisasi/badan di mana penyelidikan dijalankan)

TIDAK TERHAD

Disahkan oleh:

(TANDATANGAN PENULIS)

(TANDATANGAN PENYELIA)

Alamat Tetap:

110 TAMAN NURI
JALAN DATUK KUMBAR
05300 ALOR STAR
KEDAH

MOHAMAD MAZWAN MAHAT
(Nama Penyelia)

Tarikh: **24 NOVEMBER 2009**

Tarikh: : **24 NOVEMBER 2009**

- CATATAN:
- * Potong yang tidak berkenaan.
 - ** Jika tesis ini SULIT atau TERHAD, sila lampirkan surat daripada pihak berkuasa/organisasi berkenaan dengan menyatakan sekali tempoh tesis ini perlu dikelaskan sebagai atau TERHAD.
 - ♦ Tesis dimaksudkan sebagai tesis bagi Ijazah doktor Falsafah dan Sarjana secara Penyelidikan, atau disertasi bagi pengajian secara kerja kursus dan penyelidikan, atau Laporan Projek Sarjana Muda (PSM).

NUMERICAL INVESTIGATION ON THE EFFECT OF DIFFERENT STRUT
ANGLE TO THE CEREBRAL ANEURYSM

NOOR HARLIANA BINTI A.HAMID

Report submitted in partial fulfilment of the requirements
for the award of the degree of
Bachelor of Mechanical Engineering

Faculty of Mechanical Engineering
UNIVERSITI MALAYSIA PAHANG

NOVEMBER 2009

UNIVERSITI MALAYSIA PAHANG
FACULTY OF MECHANICAL ENGINEERING

We certify that the project entitled “*Numerical Investigation on the Effect of Different Strut Angle to the Cerebral Aneurysm*” is written by *Noor Harliana bt A. Hamid*. We have examined the final copy of this project and in our opinion; it is fully adequate in terms of scope and quality for the award of the degree of Bachelor of Mechanical Engineering. We herewith recommend that it is accepted in partial fulfillment of the requirements for the degree of Bachelor of Mechanical Engineering.

Mr Muhamad Zuhairi Sulaiman

Examiner

Signature

To
My parents and my family

A.Hamid bin Taha
Nashihah binti Idris
Nashrul Harzummy bin A.Hamid
Noor Hartiny binti A.Hamid
Noor Haryanty binti A.Hamid

for their tireless sacrifice, love and cheerful encouragement.

SUPERVISOR'S DECLARATION

We hereby declare that we have checked this project report and in our opinion this project is satisfactory in terms of scopes and quality for the award of the degree of Bachelor of Mechanical Engineering.

Signature :

Name of Supervisor : Mr Mohamad Mazwan bin Mahat

Position : Lecturer

Date :

STUDENT'S DECLARATION

I hereby declare that the work in this report is my own except for quotations and summaries which have been duly acknowledge. The report has not been accepted for any degree and is not concurrently submitted for award of other degree.

Signature :

Name : Noor Harliana binti A.Hamid

ID Number : MA06073

Date :

ACKNOWLEDGEMENT

In the name of Allah s.w.t, the most Gracious, the Ever Merciful Praise is to Allah, Lord of the Universe and Peace and Prayers be upon His final prophet and Messenger Muhammad s.a.w.

I wish to express my sincere thanks to my supervisor, Mr. Mohamad Mazwan, for his guidance, advice and support throughout the entire course of this project. His valuable insights and encouragement have become an impact to my academic life and this project. My sincere thanks go to the committee members for their valuable advice and comments for my thesis. Without them, this work would not be completed.

Last but not least, I would like to express my sincere thanks to my parents, A.Hamid bin Taha and Nashihah bt Idris, also to my family, for their infinite support, love, patience and understanding throughout my entire education. The love and support that they have shown me throughout my life has been incredible, and they have always had the wisdom to know when I still needed a helping hand, and when they should step back and let me succeed or fail on my own. For everything you have done for me, my thanks, and my love.

For all of that, I am very thankful to the co-operation and contribution from everyone that has driven me to accomplish of this project. There is no such meaningful word then...May Allah Bless you all.

ABSTRACT

The objective of this study was to determine the correlation of stent strut angle to blood flow and also to determine the flow behavior in stented aneurysm. The computational fluid dynamics was applied to access the changes of velocity and pressure in aneurysms. For this study, there are five stent with the same design but different in strut angle of the stent. The strut angle used in this study was 30°, 35°, 35°, 40°, 45° and 50°. By using 30° of strut angle as the control model and the other angle as the experimental model, there are referred to as type I, type II, type III and type IV. The simulation of the model was studied under incompressible, Newtonian, viscous and non-pulsatile condition. The results for all stents analyzed in the current study showed that the stent with higher angle are more efficient than stent with lower angle. The minimum velocity increased with the placement of stent type IV which is the higher strut angle. Meanwhile, for the pressure distribution of all type of stents indicate that lowest peak pressure obtained by stent type III. Therefore, strut angle used should be suitable to satisfy the requirement of lowest peak pressure and highest minimum velocity. So, the strut angle has to be maintained within a certain range, which varies from 40° to 45°. Finally, the correlation obtained from this numerical result could be used to investigate the pressure distribution around the aneurysms.

ABSTRAK

Objektif kajian ini adalah untuk menentukan perhubungan sudut di antara stent terhadap aliran darah dan juga untuk menentukan aliran darah . Program dinamik bendalir tiga dimensi telah digunakan untuk mengakses perubahan halaju dan tekanan dalam aneurism. Untuk kajian ini, terdapat lima stent yang mempunyai rekabentuk sama tetapi berbeza sudut di antara stent. Sudut yang digunakan dalam kajian ini adalah 30° , 35° , 40° , 45° dan 50° . Dengan menggunakan sudut 30° sebagai model kawalan dengan yang selebihnya sebagai model eksperimen, ianya dirujuk sebagai stent jenis I, jenis II, jenis III dan jenis IV. Simulasi model dikaji dengan parameter aliran mampat, Newtonian, bendalir likat dan keadaan tiada denyut. Keputusan untuk semua stent yang dianalisis menunjukkan stent yang mempunyai sudut yang lebih besar adalah lebih efisien berbanding stent yang bersudut kecil. Halaju minimum ditingkatkan dengan implant stent jenis IV di mana ianya stent yang bersudut paling besar. Walau bagaimanapun, taburan tekanan untuk semua stent menunjukkan tekanan puncak terendah dihasilkan oleh stent jenis III. Oleh itu, sudut di antara stent harus sesuai untuk memenuhi kehendak tekanan puncak terendah dan halaju minimum tertinggi. Justeru, sudut di antara stent harus dikekalkan dalam satu julat iaitu dari 40° hingga 50° . Perkaitan diperolehi dari kajian ini boleh dimanfaatkan untuk lanjutan taburan tekanan disekitar aneurism.

TABLE OF CONTENTS

	Page
SUPERVISOR'S DECLARATION	ii
STUDENT'S DECLARATION	iii
ACKNOWLEDGEMENTS	iv
ABSTRACT	v
ABSTRAK	vi
TABLE OF CONTENTS	vii
LIST OF TABLES	ix
LIST OF FIGURES	x
LIST OF SYMBOLS	xii
LIST OF ABBREVIATIONS	xiii
CHAPTER 1 INTRODUCTION	
1.1 Brain Attack	1
1.1.1 Structure of the brain arteries	1
1.1.2 The organization of brain arteries	2
1.2 Aneurysm	3
1.3 Stent	8
1.4 Stent Technology	10
1.4.1 Drug-eluting stents	11
1.4.1.1 Sirolimus-eluting stents	11
1.4.1.2 Paclitaxel-eluting stents	11
1.4.1.3 Other drug-eluting stents	12
1.4.2 Covered stents	12
1.4.3 Bifurcated stents	12
1.4 Objectives and Scopes	13
CHAPTER 2 LITERATURE REVIEW	
2.1 Flow behavior in aneurysm	15
2.1.1 Experimental investigations of aneurysm flows	16
2.1.2 Flow behavior in cerebral aneurysm	18
2.2 Flow in stented aneurysm	22

CHAPTER 3 METHODOLOGY

3.1	Computational Fluid Dynamics	30
3.2	Simulation Detailed	
3.2.1	The software	32
3.2.2	Geometry of the model	32
3.2.3	Geometry of the stent	33
3.2.4	Governing equation of blood flow	36
3.2.5	Assumption parameter and boundary condition	36
3.2.6	Finite Volume Method	37

CHAPTER 4 RESULTS AND DISCUSSIONS

4.1	Results	38
4.2	Velocity Profile	38
4.3	Pressure	47

CHAPTER 5 CONCLUSION AND RECOMMENDATIONS

5.1	Conclusion	56
5.2	Recommendations	57

REFERENCES	58
-------------------	----

APPENDICES	61
-------------------	----

A1	Data for pressure of blood flow with stent
A2	Data for velocity of blood flow with stent

LIST OF TABLE

Table No		Page
1.1	Types of aneurysm	5
1.2	General shape of aneurysm	6
1.3	Types of stent	10
2.1	Comparison of maximal mean values of velocity, vorticity and strain rate fields at both peak systole and peak diastole	27
4.1	Minimum velocity for all types of strut angle	41
4.2	Percentage of minimum velocity for all types of stent strut angle	42
4.3	Data for two points in streamlines	51
4.4	Peak pressure for all type of strut angle	52

LIST OF FIGURES

Figure No		Page
1.1	Structure of normal brain artery	2
1.2	Circle of Willis	3
1.3	Techniques for treating a brain aneurysm	8
2.1	Stream lines on intracranial aneurysm	19
2.2	Pressure distribution (ruptured)	20
2.3	Pressure distribution (unruptured)	20
2.4	Blood in aneurysm (unruptured)	21
2.5	Blood in aneurysm (ruptured)	21
2.6	Flow pattern variation due to the stent	23
2.7	Schematic diagram shows the effect of flow pattern in the aneurysm sac downstream from the parent vessel	24
2.8	Comparison of velocity fields at peak systole corresponding to the control model and experimental models	26
2.9	Patient-specific image based simulations of hemodynamics before and after aneurysm stenting	29
3.1	Flow Chart	31
3.2	Geometry model of stent	32
3.3	Geometry model of aneurysm with stent	33
3.4	Stent with 30° of strut angle	34
3.5	Stent with 35° of strut angle	34
3.6	Stent with 40° of strut angle	34
3.7	Stent with 45° of strut angle	35

3.8	Stent with 50° of strut angle	35
4.1	Velocity profile in aneurysm region	40
4.2	Percentage of velocity for 4 types of strut angle	43
4.3	Velocity bandwidth for each type of stent	43
4.4	Stented Aneurysm Model	44
4.5	Stent with 30° strut angle velocity streamlines	44
4.6	Stent with 35° strut angle velocity streamlines	45
4.7	Stent with 40° strut angle velocity streamlines	45
4.8	Stent with 45° strut angle velocity streamlines	46
4.9	Stent with 50° strut angle velocity streamlines	46
4.10	Pressure distribution for all stented aneurysm	48
4.11	Flow direction in aneurysm region	51
4.12	Correlation of peak pressure for all types of strut angle	53
4.13	Stent with 30° strut angle pressure streamlines	53
4.14	Stent with 35° strut angle pressure streamlines	54
4.15	Stent with 40° strut angle pressure streamlines	54
4.16	Stent with 45° strut angle pressure streamlines	55
4.17	Stent with 50° strut angle pressure streamlines	55

LIST OF SYMBOLS

u_i	velocity in the i -th direction
P	pressure
f_i	body force
ρ	density
μ_i	viscosity
δ_{ij}	Kronocker delta

LIST OF ABBREVIATIONS

3DRA	Three-dimensional rotational angiography
CFD	Computational Fluid Dynamics
CT	Computer-assisted tomographic
DSA	Medical subtraction angiography
FEFLO	Incompressible flow solver
GTA	Computer tomographic angiography
ICA	Intracranial aneurysm
ISR	In-stent restenosis
LBM	Lattice-Boltzmann Method
LDV	Laser-Doppler velocimetry
MRA	Magnetic resonance angiography
MRI	Magnetic resonance Imaging
PIV	Particle-image velocimetry
PTFE	Polytetrafluoroethylene
PTV	Particle-tracking velocimetry
SPH	Smooth-particle hydrodynamics
WSS	Wall shear stress

CHAPTER 1

INTRODUCTION

1.1 BRAIN ATTACK

A “brain attack” is the brain version of heart attack and it occurs when blood circulation to the brain fails. Brain cells can die from decreased blood flow and the resulting lack of oxygen. There are two broad categories of stroke: those caused by a blockage of blood flow and those caused by bleeding. The most frequent cause of loss of blood supply to brain tissue is atherosclerosis. However, blood supply may be lost due to another important reason: a ruptured blood vessel. When a brain aneurysm ruptures, the blood flowing in the parent artery from which the aneurysm arose is suddenly no longer flowing to the nerves and other cells that make up normal brain tissue; in effect, this blood now gushes out into the subarachnoid space. The region of brain which has once been supplied by that parent artery whose aneurysm has now burst becomes ischemic, and may thereafter become infarcted.

1.1.1 Structure of the brain arteries

Brain arteries can be likened to steel cylindrical pipes, each consisting of a wall enclosing a hollow space. The larger brain arteries run in a space on the surface of the brain known as the subarachnoid space.

The wall of a brain artery is comprised of three major layers and the total of six main components. The three main layers of an artery are the intima, the media and the

adventitia. Between the media and the intima is a thin layer of elastic tissue. This layer is referred to as the elastic lamina, and it is the only elastic layer occurring in the wall of the brain artery. The elastic layer has many naturally occurring openings (perforations) in it.

The six components of a blood vessel wall are endothelial cells, collagen fibers, elastic fibers, smooth muscle cells, fibroblasts and nerve fibers. In the smallest of the brain vessels, known as brain capillaries, there are also two other cell type, namely, astrocytes and pericytes .

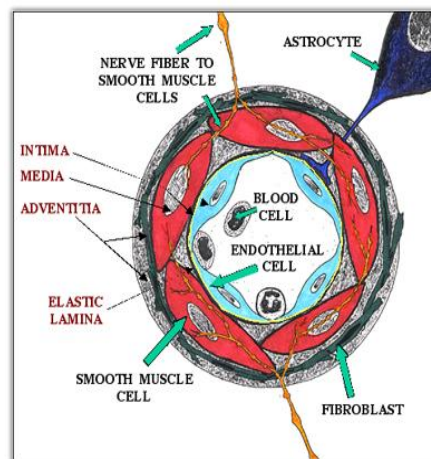


Figure 1.1: Structure of normal brain artery

Source: www.brainaneurysm.com

1.1.2 The organization of brain arteries

Brain arteries are organized as follows: from the main pipes that enter into the brain, a ring from the arteries arises that encircles the under surface of the brain. This ring is known as ‘Circle of Willis’.

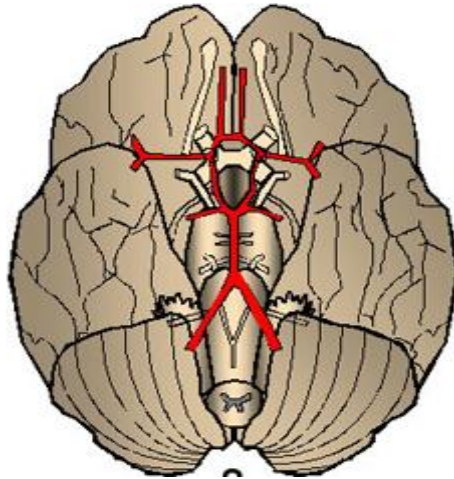


Figure 1.2: Circle of Willis

Source: www.brainaneurysm.com

Figure shows the under-surface of the brain. The major arteries in this region are shown in red. Together they have formed a ring-like structure called the 'Circle of Willis', a critical point of communication between the main arteries supplying the substance of the brain. The front part of this group of arteries is referred to as the 'anterior circulation'; the back part is referred to as the 'posterior circulation'. All of these arteries lie in the 'subarachnoid space' (SAS), a space normally filled with circulating cerebrospinal fluid.

1.2 ANEURYSM

The most common pathology that usually found in human arteries and some primates is the aneurysm. The intracranial aneurysm is generally found in females than in males. [1] These intracranial aneurysms mostly not rupture if their diameter is less than 10mm. But for cerebral aneurysms, if their size is roughly larger than 5 mm in diameter, it is considered as a critical. The rupture of an intracranial aneurysm will resulting subarachnoid hemorrhage that is serious events and it associated with high rates of mortality and morbidity. [1]

There are some types of aneurysms that can occur in the body. There are about four different types of aneurysm which is thoracic aortic aneurysm, abdominal aortic aneurysm, cerebral aneurysm and peripheral aneurysm. It can be simplified in Table 1.

It should be noted that there are different several types of cerebral aneurysm. They are being classified through the involving layers of the wall. There are two most recognized shapes of aneurysms which is 'saccular' and 'fusiform'. The third shape, 'mycotic' are also recognized but it is much rarer than the other two. These three shapes of aneurysms is an expansion of a blood vessel wall involving all layers of the wall. It can be shown in Table 2.

The role of genetic factors will lead to the intracranial aneurysms, but other factors, such as hemodynamic stress at arterial bifurcations, congenital medical defects, degenerative artery wall changes, smooth muscle cell apoptosis, smoking and excessive alcohol consumption are also the factors that contributed to aneurysmal development.[1] The changes of the aneurysmal wall are already advanced or have been modified with other factors once it is detected. Therefore, it will know the details on how they originate, grow and rupture.

Cerebral arteries are muscular arteries that having significantly less elastin in the media (than elastic arteries) and lacking the external elastic lamina. Most bifurcations of the cerebral vasculature are structurally stable, but a small number develop a weakness that causes the wall to expand outwardly in the region near the flow divider of the branching artery.

Table 1.1: Types of aneurysm

(Source: <http://www.nhlbi.nih.gov>, <http://www.mayoclinic.org>)

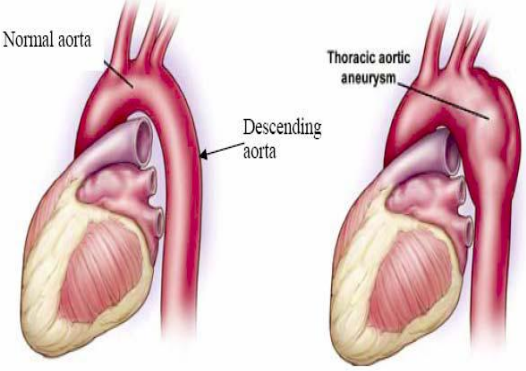
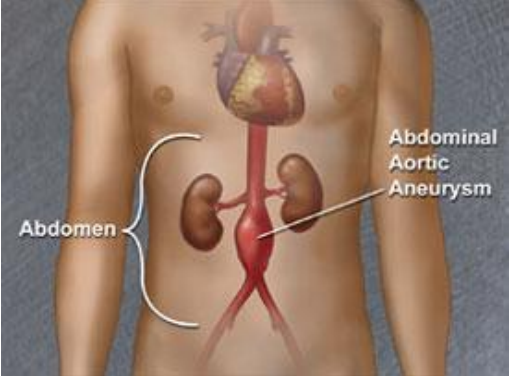
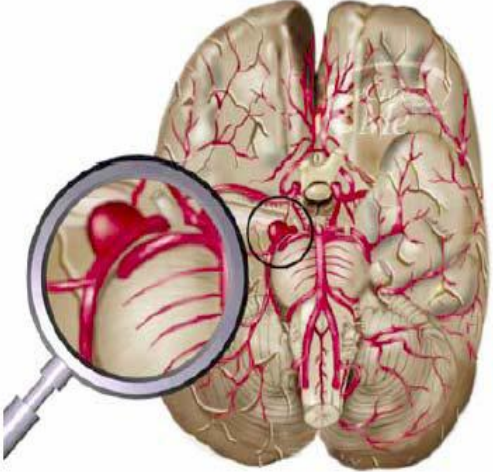
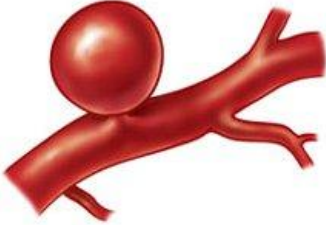
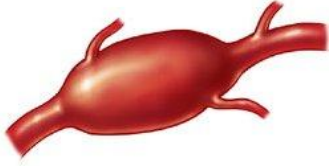
Types of aneurysm	Figure
Thoracic Aortic	 <p>The figure consists of two anatomical diagrams of the human heart and aorta. The left diagram shows a normal aorta with labels for 'Normal aorta' and 'Descending aorta'. The right diagram shows a thoracic aortic aneurysm, with a label for 'Thoracic aortic aneurysm' pointing to the enlarged section of the aorta in the chest area.</p>
Abdominal Aortic	 <p>The figure shows a human torso from the chest to the waist. The heart is visible in the chest, and the abdominal aorta is shown descending. A label 'Abdomen' is on the left, and 'Abdominal Aortic Aneurysm' is on the right, pointing to a bulge in the abdominal aorta. The kidneys are also visible on either side of the aorta.</p>
Cerebral	 <p>The figure shows a human brain with a network of cerebral arteries. A magnifying glass is positioned over a specific area of the brain, highlighting a cerebral aneurysm. The brain is shown in a frontal view, and the arteries are colored red.</p>

Table 1.2: General shape of aneurysm

(Source: <http://www.discuss.com.hk>)

No	Shape of Aneurysm	Figure
1	Saccular	 Saccular Aneurysm
2	Fusiform	 Fusiform Aneurysm

Hemodynamic stress at certain points of the arterial tree might be an important factor in both triggering aneurysm growth and leading to rupture of an existing aneurysm. Medical imaging technique, such as medical subtraction angiography (DSA), computer tomographic angiography (CTA) or magnetic resonance angiography (MRA) are now capable of providing more accurate three-dimensional information on intracranial vessel geometry.[4]

The gold standard for detection of a brain aneurysm is cerebral angiography. Here, a contrast dye is first injected through a catheter device inserted usually in a thigh (femoral) artery. From here, the dye is eventually enters one or more of the main brain arteries, where it is X-ray imaged. It typically provides a detailed roadmap of the brain circulation. An aneurysm appears as an expansion of the vessel. If there is no clot (thrombus) in the aneurysm, it will light up like a sac coming off the parent artery. If the lumen (or inner space) of the brain aneurysm is packed with clot (this is more common

in bigger brain aneurysm due to slowing of blood flow in the lumen), then sometimes the real extent of the brain aneurysm is may not seen by this method.

Other X-ray based advanced imaging methods for detecting brain aneurysm are magnetic resonance imaging (MRI) and its associated method referred to as magnetic resonance angiography (MRA). The advantages of these method are that they are less invasive than cerebral angiography, in that they do not involve femoral (thigh) artery puncture and insertion and navigation of a long catheter through the arteries. However, they may not detect the smallest of brain aneurysm as well as cerebral angiography can, and are not able to be used in certain patient in whom metallic hardware has been placed.

Ordinary computer-assisted tomographic (CAT or CT) scanning with a limited injection of contrast dye is another way to detect brain aneurysm, but not a very good way (note that without injection of contrast, an ordinary CT scan is almost useless unless the brain aneurysm is very large, calcified and ruptured). Even when used as part of CT angiography, this method is not as sensitive or as specific compared with cerebral angiography.

If a brain aneurysm is detected, but hasn't ruptured, the choice of treatments is very controversial at the moment. Some physicians have found that a brain aneurysm diameter (size) of 10mm may be the critical number after there is a significantly increased risk of brain aneurysm rupture. Other, however, have found that rupture occurs in even smaller brain aneurysms (3 to 6mm in diameter) and therefore advocate that the 10mm size 'threshold' is not valid for determining risks and deciding on close observation versus actual treatment. The bottom line is that each case of brain aneurysm should be treated on an individualized basis, taking into the consideration the age of the patient, copresence of significant medical conditions, the site and size and shape of the brain aneurysm, whether there is a history of previous aneurismal hemorrhage in the patient, the experience of the treating physician and surgeon, and the type and risk(s) of treatment option most suitable for that brain aneurysm and person. There are some techniques for treating a brain aneurysm as shown in Figure 1.7. Firstly shows a directly

clipped across brain aneurysm neck, thereby effectively removing the brain aneurysm from the circulation. Second figure shows a trapping of a brain aneurysm, with surgical clips being placed on the artery sections and draining brain aneurysm. Last figure shows a hollow stent (S) being placed by catheter across the region of the vessel that opens into the lumen of the brain aneurysm.

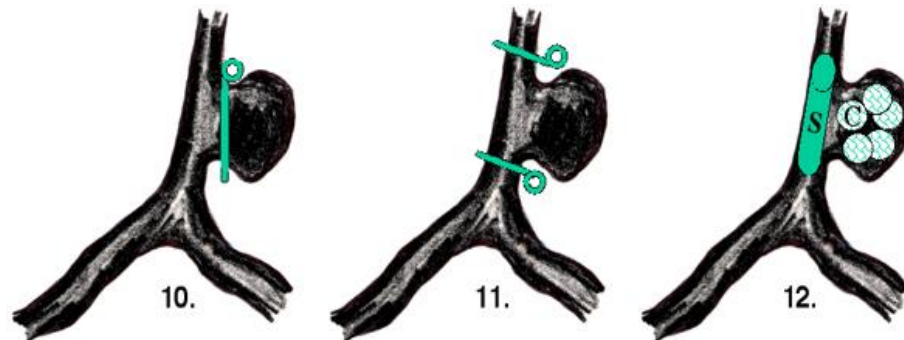


Figure 1.3 Techniques for treating brain aneurysm

Source: www.brainaneurysm.com

1.3 STENT

At present, the market of stent is increasing rapidly as a method of reopening the clogged blood vessels of the legs and heart. It is because of their high initial success rate, minimal invasive nature and improved long-term effectiveness than the other method. There are three most common treatment for vascular disease which does not respond to pharmacologic therapy are vascular bypass grafting, percutaneous transluminal balloon angioplasty and percutaneous transluminal stenting with the aid of balloon angioplasty.[2]

At the turn of the 20th century, one of the scientific breakthroughs is the introduction of the drug-eluting stent, also known as drug-coated stent. With the technological advancement in engineering and design, drug-coated stent has become as

ultimate device in treating cardiac vascular disease. As a result, other stent parameters are taken lightly and considered less important by many specialists. The underappreciation of the stent design, that has evolved for the past 18 years, will affect the overall performance of the stent. The structural, geometry and dimension play a crucial role in the delivery process, performances of the stent and the procedural success.

The stent was introduced to replace the traditional invasive surgery and angioplasty balloon that was used in treating cardiac vascular disease. In the early stage of angioplasty, cardiologists use a balloon to expand the artery that is clogged. However, in some cases the wall of the coronary artery becomes weakened after the balloon is dilated, resulting in an acute or subacute collapse of the artery. The stent was created in the 1980s in response to the danger posed by the angioplasty balloon. The stent was able to diminish the danger of collapsing artery wall, but it gave birth to the problem of restenosis. After years of engineering and design, the stent is equipped with biocompatible and radio visible coating to reduce restenosis. The coating on the stent is not only the factor that is responsible for today's stent performance and success in procedures, but many other stent parameters.

A stent that is inserted into a vascular which it features either an expandable wire or perforated tube is to avoid a disease-induced localized blood flow constriction.[2] This technique is viewed as a minimally invasive treatment and a very promising alternative or complement to more traditional approaches such as coils and surgery. [4] However, the optimal design for the stent structure is dependent on the specific location and type of aneurysm. Issues with respect to the design of vascular stents include maximal radial stiffness, maximal flexibility, minimal foreshortening, minimal dogboning, minimal longitudinal recoil, minimal coverage area, maximal fatigue durability.

Particularly, foreshortening driven from unfavorable shearing between the stent and the vascular or dogboning induced from penetration at the edges of the stent, can be a primary cause of potential limitations such as restenosis. Thus, new stent design should focus on features related to mechanical performances while considering the other issues described above to mechanical characteristics.[4]

It is commonly accepted that the shear rate at the wall affect the aggregation of blood platelets, as well as the reactions that lead to coagulation. Therefore, the ideal stent would be that which would optimize the coagulation process and would reduce the pressure on the aneurism wall. Thus, the stent would modify the blood circulation in the aneurysm but not to stop it. An impermeable stent will prevent the blood to bring new material to coagulation region and, may also suppress flow in secondary vessels, or at a bifurcation. [4]

Stent may be classified based on their predeployed repeating ‘cell’ pattern of metal constructions and the nature of the stent delivery system. Recently, a stent classification system which based on structural characteristics of the stent is summarized on the Table 3.

Table 1.3: Types of stent

Type	Example
Self Expanding	Wallstent, Radius
Balloon Expanding	Gainturco-Roubin, Crossflex LC
Tubular Stents	MultiLink, Crown, NIR, Bestent, Terumo
Hybrid Stent	GFX, InFlow Goldflex
<i>Coil Stent</i>	Crossflex, Wiktor

1.4 STENT TECHNOLOGY

Following the first clinical application of a coronary stent in 1986, the implementation of the coronary stents has become an integral part of more than 80% of percutaneous coronary interventions. Multi-centre trials have demonstrated sustained

benefit combined with effective anti-platelet therapy, which has led to the widespread use of coronary stents.[8] Coronary stents are evolving in both composition and design.

New stent technology is driven by clinical requirements, and particular influences are restenosis and anatomical challenges. Specialized design for bifurcations lesions and saphenous vein grafts are being developed. However, the most widely applicable advance has been with drug-eluting stents for the prevention of in-stent restenosis (ISR). But there is the latest stent technology for specific anatomic lesion subsets and the prevention of ISR, including coated, covered and dedicated bifurcation stents.[8]

1.4.1 Drug-eluting stents

The most significant limitation of current coronary stenting is the need for repeat procedures. Trials comparing multi-vessels stenting and coronary artery bypass surgery have found a 16% absolute increase in the risk of requiring repeat revascularization at 1-year follow up, due primarily ISR. While brachytherapy has been developed to prevent repeat restenosis, local pharmacological treatments with drug-eluting stents have been shown to prevent initial neointimal proliferation. The most widespread clinical experience has been established with the Sirolimus-eluting Bx velocity stent (Cypher, Cordis, Johnson & Johnson) and the paclitaxel-eluting NIR (Medinol) and express (Boston Scientific) stents.

1.4.1.1 Sirolimus-eluting stents

Sirolimus (rapamycin) which is an immunosuppressive agent used to prevent transplant rejection, has potent anti-migratory effects on smooth muscle cells. Clinical trials have determined that sirolimus is an effective local inhibitor of restenosis. Ongoing studies are evaluating the use sirolimus-eluting stents for the treatment of ISR.

1.4.1.2 Paclitaxel-eluting stents

Paclitaxel (Taxol) is a microtubule-stabilising agent used in chemotherapy of many common solid tumors, and has activity in preventing neointimal proliferation.

Initial clinical experience with the local delivery of paclitaxel by the drug-eluting Express stent was in the TAXUS I trial.

For the treatment of ISR with paclitaxel-eluting stents, only uncontrolled data are available. In the TAXUS III trial, 28 patients with ISR were treated with one or more paclitaxel-eluting NIR stents. The angiographic restenosis rate was 16% at 6-months, and tended to occur at gaps between paclitaxel-eluting stents. The TAXUS V trial is an ongoing prospective trial of the paclitaxel-eluting Express stent compared with beta brachytherapy for the treatment of ISR.

1.4.1.3 Other drug-eluting stents

Other stents that have been studied include the Everolimus (sirolimus analogue)-coated stent, the dexamethasone-coated Dexamet stent and the paclitaxel-coated Achieve stents.

1.4.2 Covered Stents

Biocompatible, covered stents were first used in peripheral arterial disease, mainly for aneurysm or vascular repair following perforation. Many different coverings have been studied including autologous venous and arterial grafts. However, the most widely studied covered stent is the polytetrafluoroethylene (PTFE)-covered Jostent (Jomed). The Jostent coronary stent graft has a thin layer of PTFE placed between two stainless steel stents and was initially introduced to treat native coronary artery aneurysms and coronary perforations.

In coronary aneurysms, a case series of seven patients reported successful placement of PTFE covered stents without complication.

1.4.3 Bifurcated stents

Coronary artery disease commonly occurs at bifurcations, secondary to flow pattern. These lesions are technically challenging and commonly result in side-branch occlusion and a higher rate of restenosis. Several techniques use conventional stent in

bifurcations lesions and include: T-stenting, Y-stenting and the culotte method. These method have variable success and often require further intervention. Stents designed specifically for bifurcations lesions increase access to side branches, decrease procedure time and potentially improve clinical outcomes.

The Multi-Link Frontier stent (Guidant) and Nirside stent (Medinol) are other dedicated bifurcations stent that are being assessed in non-randomised, safety studies. In addition to the specialized designs for bifurcating stents, 85 patients have been treated with one or two CYPHER stents (Johnson & Johnson), the majority of which were T-stents.

Advanced in coronary stent technology has markedly improved procedural success, safety and both acute and chronic outcomes. Evolving technology in stent design will lead to expanded indications and better prognosis. Ongoing trials will address the impact of newer stent technologies on the treatment of complex lesions, bifurcations lesions, small-diameter vessels, multi-vessel disease, ISR and left main disease.

1.5 OBJECTIVES AND SCOPES

Many researches have been study on the aneurysm growth until it ruptures. With the technological advancement in engineering and design, the implementation of stent becomes more popular as a treatment of aneurysm. The performance of the stent depends on its geometry and design. There are some parameters that need to be considered in order to design the best stent that will give good performance. Previous studies have performed the analysis on effect of void area of the stent, effect of double layer stent and so on.

The objective of this project is to determine the correlations between stents structural parameters and blood flow. The parameter considered in this project is different strut angle of the stent. This project also considered to determine the flow behavior in stented aneurysm.

The scopes are to analyze selected stents based upon different strut angle parameters. Based on the different strut angle used, the correlation between strut angle and the blood flow can be obtained. Application of stent will be on fixed aneurysm. In this project, we will apply the stent to the fusiform aneurysm only. For the analysis, we used computational fluid dynamics to access the changes of velocity and pressure in aneurysms. Non pulsatile blood flow will be used in the simulation. Solutions will be based on numerical approach only.

CHAPTER 2

LITERATURE REVIEW

2.1 FLOW BEHAVIOR IN ANEURYSM

Blood flow in an aneurysm generally depends on its geometric configuration and relation to the parent vessel, the size of the orifice and the volume of the aneurysm. The classical treatments of aneurysms are direct surgical clipping or endovascular coil insertion which decides by the size of the aneurysm. However certain intracranial aneurysm are not easy to be carried out at some special complex structure; fusiform, wide-neck, giant size and involvement branch vessel etc. Hence, hemodynamic factor such blood velocities, wall shear stress (WSS), and blood pressure plays an important roles in the pathogenesis of aneurysms.

There have been several research efforts to investigate the problems using numerical simulation. There are basically two approaches: using artificial models which are supposed to reflect the important geometrical and flow characteristics of the aneurysm and working the real models derived from medical imaging techniques. In the case of artificial models the researcher has complete freedom in preparing the geometry and the numerical mesh. Because of relative simplicity, regularity and controllability of the geometry the mesh has usually a good quality. Examples for such artificial geometries are abdominal aneurysm [23], abdominal aortic branches [27], intracranial aneurysms.[4]

In the second approaches the arterial geometry is obtained on a digital format consisting of voxels. It is possible to perform simulations on this mesh consisting of small cubes but this have a rough appearance since the surfaces of all cubes are in one of the three coordinates direction. In this case, especially near the wall, the results will be unrealistic.

For that reason, factors that leading to aneurysm growth and rupture which is not clear. Many authors emphasize the potentially key role of the wall shear stress. However, there is considerable among researchers whether the high or the low values, or the oscillation of the shear are to blame. To the best knowledge of the authors, there is no convincing evidence supporting any of these hypotheses.

From the findings, they reported about 20 processed cases which all have more or less similar geometries. Out of these cases three have ruptured. They identified three groups of aneurysm, according to the locations of maximum shear stress. They tried to relate the aspect ratio of the sac with the wall shear stress but found only a weak correlation. No significant correlation has been found between the magnitude of shear stress and the possibility of rupture. [26]

The simulations on the sidewall aneurysm with curved parent vessel found that the flow pattern varies during the cycle with reverse flow in diastole near the aneurysm. Based on this they hypothesised a mechanism of aneurysm growth – namely that at the location of largest shear stress oscillation vessel wall is weakened and the aneurysm is prone to grow. [24]

2.1.1 Experimental Investigations of Aneurysm Flows

Similar to computational studies, there are two approaches to building flow models of aneurysm: simplified models and scaled-up real models extracted from angiography data. The models are usually made of transparent acrylic or Perspex blocks. Laser-based optical methods are almost exclusively used since the flow field is very complicated and the usage of intrusive probes would not only be cumbersome but

also disturb the flow while providing much less information. To avoid unwanted refraction at curves surface refractive index matching techniques are used. One of the central questions of these experiments is to determine to what extent the qualitative flow pattern changes during the cardiac cycle. The results are controversial and it is very likely that the answer is largely influenced by the exact shape of the unsteady input flow function.

From the investigation of flow field with particle tracking velocimetry (PTV) and by the means of flow visualization for varying curvature for the parent vessel, they concluded that intra-aneurysm velocities increase with increasing curvature. They also found that the qualitative appearance of the flow field is affected. They also measured velocity field inside a model sidewall aneurysm using laser-Doppler velocimetry (LDV). They found slight variations in the inflow angle during the cycle but otherwise the flow field was similar. [25, 26]

The peak shear stress was at the distal lip and the magnitude of shear stress increased with decreasing sac size. By using PTV and flow visualization, they study the unsteady flow pattern in an (artificial) model aneurysm with and without stents. It could be expected that the average flow velocity and the shear stresses are significantly reduced with the insertion of stents. However, they obtained a surprising result. [28]

In the unstented case the flow pattern remain unchanged throughout the cycle except for the velocity magnitude. Stent deployment across the neck of the aneurysm, however, produced qualitative changes of the flow pattern during the cycle. These changes were characteristics for the particular stent design. They have reported on LDV and particle image velocimetry (PIV) measurements in a real models aneurysm. [22] Detailed time resolved flow velocities were obtained and the variation of in and outflow zones during the cycle identified. The possible zones of very low shear stress by the insertion of a stent were also determined. [29]

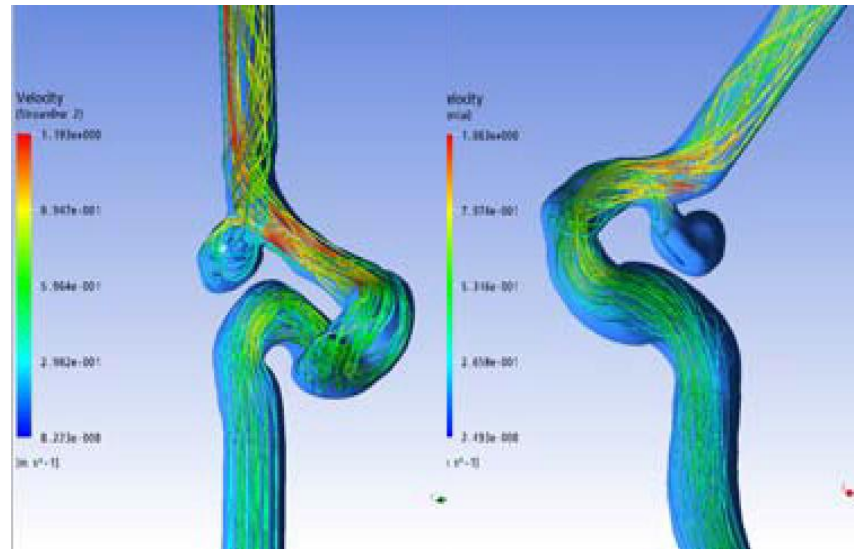
2.1.2 Flow Behavior in Cerebral Aneurysm

Flow impacts results in two physical forces different in direction. One is the ‘impacting forces’, which results from the inertial forces of the bloodstream and acts perpendicularly to the vessel wall. The other is the wall shear stress (WSS), the viscous friction of the bloodstream that acts parallel to the vessel wall. The role of formal force intuitively assumed significant in the pathophysiology of cerebral aneurysm, however, this assumption needs to be proven with scientific evidence because the site of flow impact around the aneurysm and the magnitude of the impacting force have not been obtained yet.

The impacting force of the bloodstream can be considered as the local elevation of pressure at the area of flow impact. The kinetic energy of fluid is converted to pressure when the velocity decreases and vice versa. Thus, it is called ‘dynamic pressure’ in the field of fluid mechanics. At the time of flow impact when the blood stream changes its direction, the velocity decrease momentarily, and most of the dynamic pressure is converted to the static pressure. This result in the local pressure elevation at the area of the flow impact.

The unsteady flow analyses of a ruptured cerebral aneurysm and unruptured cerebral aneurysm also been performed before. As a result, the unsteady recirculation flow were observed in the vicinity of the bleb in the ruptured case, and the results of unruptured case is shown in Figure 2.1b. The blood flows in the ruptured aneurysm is clearly observed more complex than the flow pattern inside of unruptured case. The flows in the ruptured aneurysm are not only separation, but also exists a strong swirl created in the centre of the aneurysm. [9]

The results indicate that more energy was loosed at the ruptured case when the blood flow passes the aneurysm. Furthermore, the bleb is found at ruptured case in Figure 2.1a. A high speed recirculation and flow attachment on the bleb can be also observed around the bleb edge in Figure 2.1.



a) Ruptured case

b) Unruptured case

Figure 2.1: Stream lines on intracranial aneurysm

Source : Y.Qian, 2007

Figure 2.1 shows blood stream lines which started at the section of intracranial aneurysm (ICA). Observation at the inside of the aneurysms, there are more flows passing through the aneurysm of the ruptured case. The simulation of non-aneurysm was carried at the same flow conditions as ruptured and unruptured cases. The results indicated that at the ruptured case blood takes longer time to pass into the aneurysm, then go out from the aneurysm, and the energy loss are also higher compare with unruptured case. The energy losses may be transferred to the energy of pressure and stress to load on the pathological aneurysm surfaces. The aneurysm surfaces will be drawn and shrunk frequently.

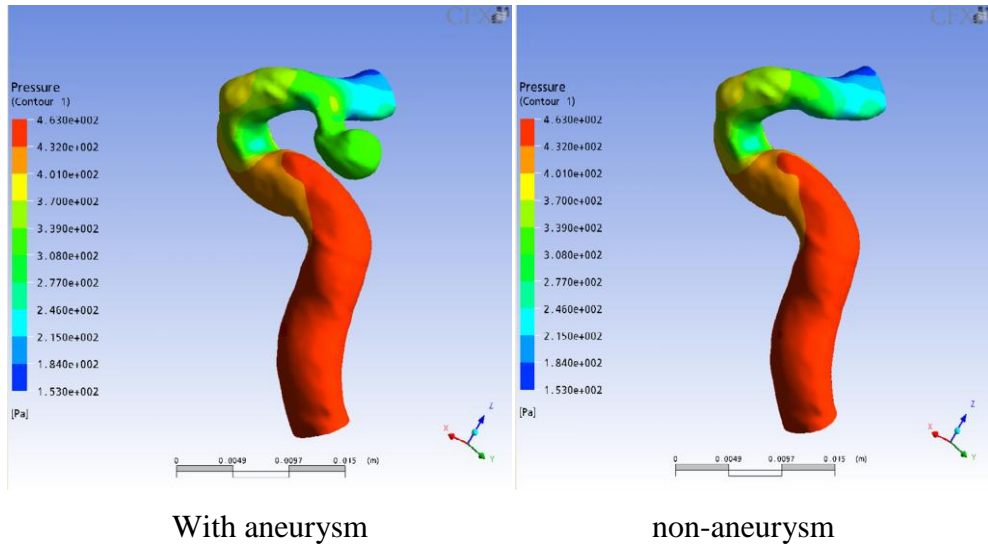


Figure 2.2: Pressure distributions (unruptured)

Source : Y.Qian, 2007

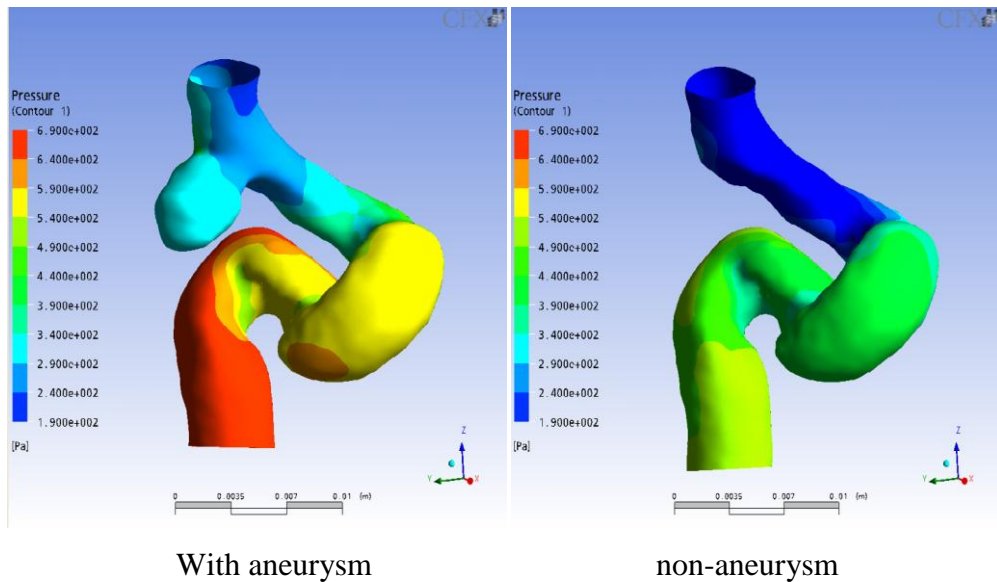


Figure 2.3: Pressure distributions (ruptured)

Source : Y.Qian, 2007

Figure 2.2 shows flow pattern at the section of the unruptured aneurysm. One vertex is observed at the top of the aneurysm, and main flows from the parent vessel are resisted at near aneurysm neck area. On the other hand, three strong vertexes can be observed in Figure 2.3. The main flows pass through the aneurysm neck and

directly move into the aneurysm top, and stagnation creates at the top of the aneurysm. The flows are separated around the stagnation point and lines, then turn into the bleb. A vortex is visualized inside the bleb.

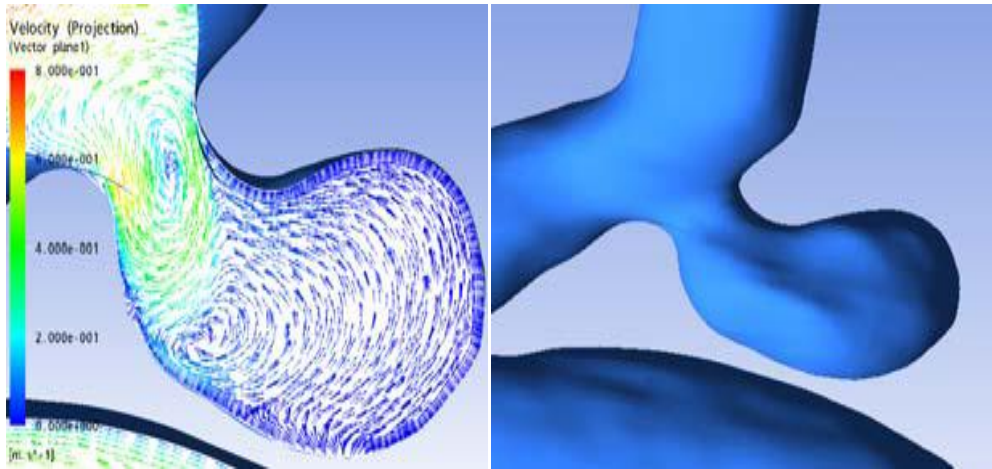


Figure 2.4: Blood in aneurysm (unruptured)

Source : Y.Qian, 2007

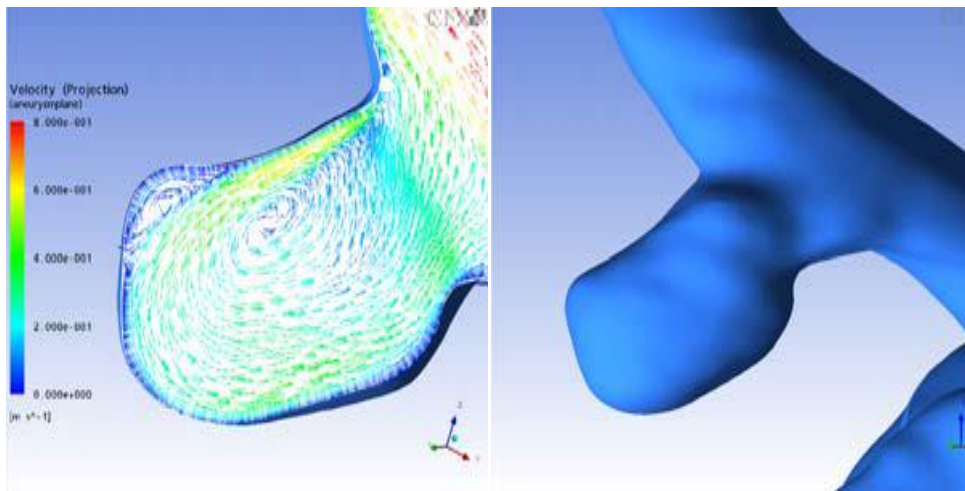


Figure 2.5: Blood in aneurysm (ruptured)

Source : Y.Qian, 2007

2.2 FLOW IN STENTED ANEURYSM

Since the first implementation of stent in humans in 1986, many improvements, changes and discoveries have occurred to make them safer and more functional. The presence of non-biological device inside an artery causes an inevitable inflammation response and influences the fluid dynamic behavior in the regions next to the arterial wall.[3] Parts of the stent struts protruding into the lumen may include the formation of vortices and stagnation zones which affect wall shear stress (WSS) spatial and temporal distribution. These effect depend on stent configuration, its global length, the delivery system, the struts dimension, shape, spacing and many others. [14,15] Moreover, low-mean shear stress, oscillating shear stress, high particle residence times, and non-laminar flow have all been shown to occur in the locations where early intimal thickening is the greatest. [16, 17, 18, 13, 20]

The new basic parameters was performed in order to understand the flow pattern in the stented aneurysm and its effect on the velocity reduction and to verify the flow reduction mechanism based on that parameters. In order to execute a qualitative analysis on the flow reduction efficiency by the stent implementation, they investigate the variation of the flow pattern in the stented aneurysm. According to the variation of the pore size and the struts position of stent, the flow pattern change.[6] Figure 2.6 shows that there are three types of flows in the stented aneurysm: (I) vortex driven by orifice flows, (II) vortex driven by aneurysm flows, (III) laminar flows driven by orifice flows. Based on these observations, the flow pattern in stented aneurysm can be classified into three groups: (I) + (III), (II) + (III) and (III). In more complex cases, they find that the vortex and the laminar flow in the aneurysm dome drive another vortex but they only consider the single vortex flow. [6]

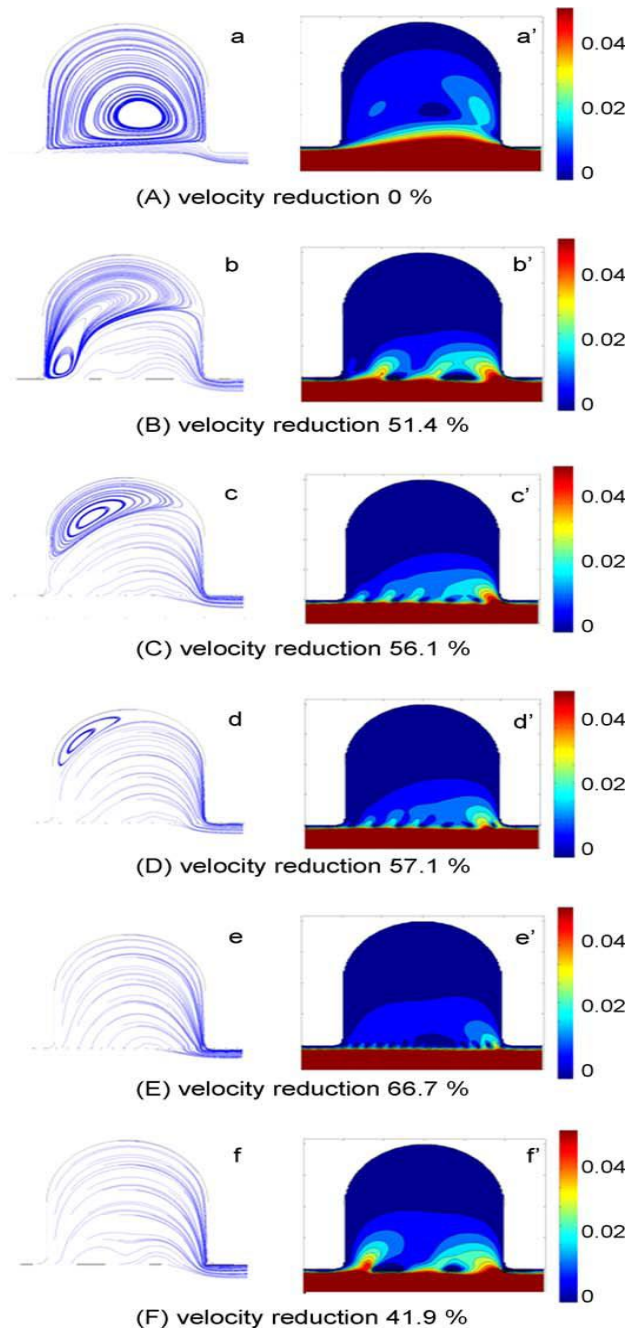


Figure 2.6: Flow pattern variation due to the stent

Source : M.Hirabayashi, 2006

On the other hand, Figure 2.6F shows that the flow pattern does not predict the velocity reduction effect directly. Figure 2.6E and F shows the same laminar flows but the velocity reduction effect is different. To know the velocity reduction effect from the flow pattern, they have analyzed the formation mechanism of the flow patterns. To

characterize the relationship between the flow pattern and the velocity reduction, they introduced new analyses on the driving flow and the driving pore. The driving flow is the inlet flow, which drives the dominant flow in the aneurysm dome and the driving pore is the inlet pore of the driving flow at the aneurysm orifice. The driving flow and the driving pore are determined by the flow pattern. Figure 2.6 suggests that the driving flow drives the dominant flow in the aneurysm dome, which determines the velocity reduction effect. The position and size of the driving pore seem to play important roles in the velocity reduction because they determine the velocity of the driving flow. [6]

The investigation on the changes in the velocity field inside the aneurysm sac as well as the hemodynamic forces within the aneurysm resulting from the implementation of one, two and three stents without the use of coils or other packing agents has been performed. From that, they observed that due to the curvature of the parent vessel, the stream diverged away from the wall before it entered the aneurysm. The stream then impinged on the distal neck of the aneurysm, splitting into two streams: a jet entering the aneurysm along the distal wall and a stream flowing through the parent vessel. (Figure 2.7)

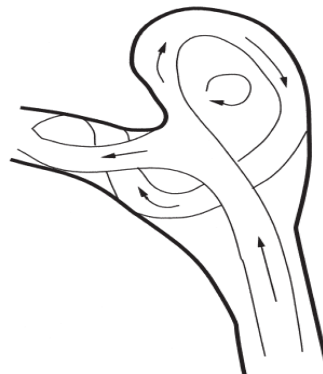


Figure 2.7: Schematic diagrams showing the effect of flow pattern in the aneurysm sac downstream from the parent vessel

Source : G.Canton, 2005

The flow rate of the fluid present in the aneurysm drastically decreased from the maximal values during the peak systole to lower values at the late stage of the systole

and at the peak diastole. This outflow merged with the main flow in the parent vessel, forming a helical vortex downstream of the aneurysm, as shown in Figure 2.7. [5]

In the model of sidewall aneurysm, the measured velocity of the jet entering the aneurysm at this plane was considerably lower than that measured in the parent vessel during most of the cardiac cycle. In fact, at any given instant of time in the cardiac cycle, the magnitude of the velocity at the entrance of the sac may reach the values measured at the proximal wall of the sac, which are 10% of the velocities in the parent vessel. Only during the deceleration phase of the systole did the magnitude of the velocity seem to reach the maximal values of 60% to 70% of the velocity of flow in the parent vessel. This maximal velocities of the jet as it entered the sac at the peak systole was consistently located at the distal half of the sac, toward the distal wall and close to the fundus, and it was concentrated in a very small area.

There were certain hemodynamic features of the velocity field that persisted after they had placed one, two or even three stents (Figure 2.8). First, the flow on the proximal wall and the fundus was nearly stagnant throughout the cardiac cycle, whereas the velocities at the distal region changed in accordance with the cardiac cycle, reaching maximal values (that decreased with number of stent) at the peak systole and minimal values (even lower than the velocities measured at the proximal wall) at the end of the cycle. Second, at the peak systole, a relatively strong vortex was always seen forming at the distal neck of the aneurysm, and the clockwise rotational motion, which was observed on the control model, remained even after the third stent had been placed. Third, during the diastole, the vortex dissipated and a near stasis was achieved inside the sac at the end of the cycle.

They also observed several important differences in the velocity field while placing the stent (Figure 2.8). The core of the vortex was predominantly located near the distal wall. Placement of one stent did not change the vortex location; however when two or three stents had been placed, the core of the vortex migrated slightly toward the center of the sac and become weaker.[5] Specifically, the presence of the third stent led to a considerably perturbed rotational motion inside the aneurysm sac and to a more random nonrepetitive pattern from cycle to cycle.

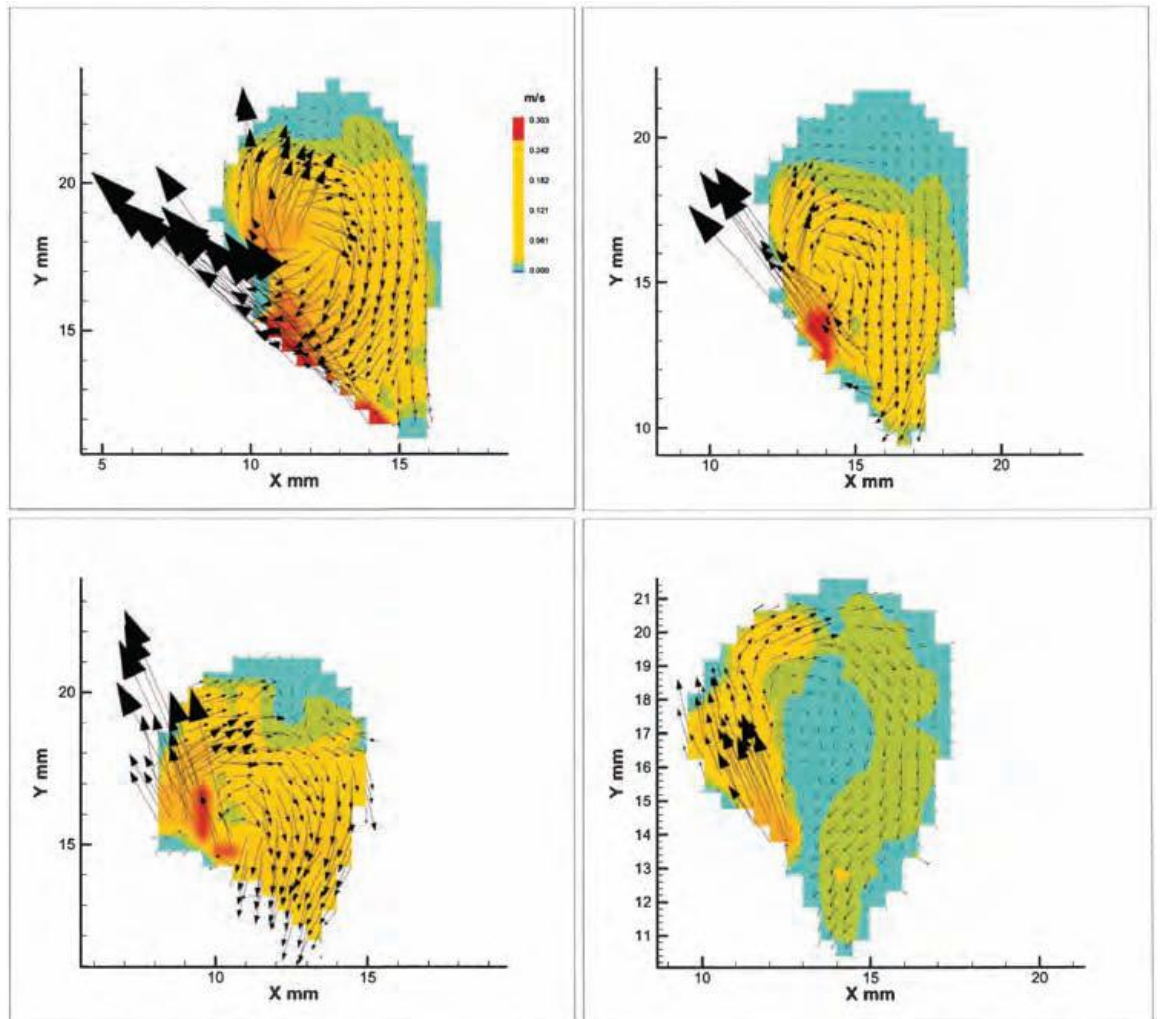


Figure 2.8: Comparison of the velocity fields at the peak systole corresponding to the control model and the experimental models.

Source : G.Canton, 2005

To provide a quantification of the effect of placing each stent, they measured the velocity field at the peak systole and at the end of the cycle and averaged them into four cardiac cycles. Table 2.1 shows a comparison of the maximal mean velocity magnitudes for the control model as well as for the experimental models after placement of one, two and three stents. At the peak systole, they measured the 40% reduction in the maximal value of the velocity after the first stent had been placed, and a 60% reduction after the third stent had been placed. This reduction was more striking at the end of the diastole,

with a 76% decrease demonstrated after the first stent had been placed and almost an 80% drop in the maximal velocity value after all three stents had been inserted.

Table 2.1: Comparison of maximal mean values of velocity, vorticity, and strain rate fields at both peak systole and peak diastole.

Variable	Velocity Magnitude (m/second)	Vorticity (1/second)	Strain rate (1/second)
Peak Systole			
Control	0.30 ± 0.011	187.07 ± 15.29	80 ± 7.76
First stent placed	0.22 ± 0.030	137.14 ± 29.40	58.70 ± 8.86
Second stent placed	0.24 ± 0.018	155.95 ± 9.02	70.25 ± 15.74
Third stent placed	0.13 ± 0.016	79.07 ± 6.49	38.39 ± 6.25
Peak Diastole			
Control	0.08 ± 0.003	34.85 ± 1.87	12.21 ± 0.70
First stent placed	0.02 ± 0.004	12.46 ± 3.48	5.47 ± 0.78
Second stent placed	0.03 ± 0.005	20.78 ± 5.18	8.38 ± 1.21
Third stent placed	0.02 ± 0.003	11.71 ± 1.76	4.72 ± 0.62

Their study represent a systematic, quantitative evaluation of the flow changes occurring inside the aneurysm as a result of placing one, two and even three stents. They compared the effect of increasing the number of stents across the neck of a sidewall aneurysm on the velocity inside the aneurysm sac. The reduction in the circulation, resulting in the implementation of the first stent could also be due to slight changes in the curvature of the parent vessel caused by the guidewire and the catheter during stent implementation, by the stent itself, or by both of implantation tools and the stent. This additional effect could be the reason for the nonlinear decrease in the circulation with placement of each consecutive stent and for the large variability observe from measurement to measurement, which was as high as 22.4%, as indicated in Table 2.1.

Considering that a decrease at the porosity of the mesh may lead to an excessive neointimal response, with a risk of secondary stenosis of the artery in a high stent metal-to-arterial tissue ratio, their result should be complemented with a clinical study that could establish the threshold for the aneurysm occlusion as well as the risk of stenosis to determine the optimal number of stent needed to prevent aneurysm growth or rupture.

The study on innovative methodology for virtual deployment of stent within patient-specific anatomical models. The methodology for virtual deployment of stents in patient specific anatomical models constructed from medical images consists of several steps; centerline extraction, host cylinder construction, stent mapping and stent adjustment. The methodology was demonstrated with an image-based model of a cerebral aneurysm that was successfully treated only with a stent.[10] The patient had a large aneurysm with a wide neck in the right internal carotid artery. The nature of this segmental injury makes it extremely difficult to treat with coils or surgical clipping techniques that are better suited for focalized injuries. Instead, the parent artery was reconstructed with a braided stent (Pipeline). Three-dimensional rotational angiography (3DRA) images were required before and after treatment and used to construct patient-specific computational models using a previously described methodology. [10]

The deployment methodology was tested in conjunction with an incompressible flow solver (FEFLO) that uses an unstructured grid embedded technique in order to model the geometry of the deployed stent inside the vascular domain. The pre-stented grid had roughly 3 million linear tetrahedral elements and a minimum resolution of 0.2 cm. After deployment of the stent, the grid was adaptively refined three times near the embedded stent in order to increase the resolution around the struts. This resulted in a mesh of approximately 15 million elements for the post-stenting case. Pulsatile flow were carried out using 'typical' flow rate waveforms measured in normal subjects and scaled to the area of the parent artery.

The result are presented in Figure 2.9. The figure shows the 3DRA image of the aneurysm before stenting (top left) demonstrating the segmental disease. The top right panel shows the stent model in its deployed state inside the parent artery. The bottom row shows the flow pattern before (left) and after (right) stenting at peak systole. It can

be clearly seen that the stent substantially diffuses the inflow jet and that the complex unsteady flow pattern of the pre-stenting case has been significantly modified into a slower, simpler and more stable flow pattern after stenting. These results are in agreement with clinical observations made with conventional angiograms obtained before and after stenting which demonstrate increased residence times and simpler flow pattern after stenting.

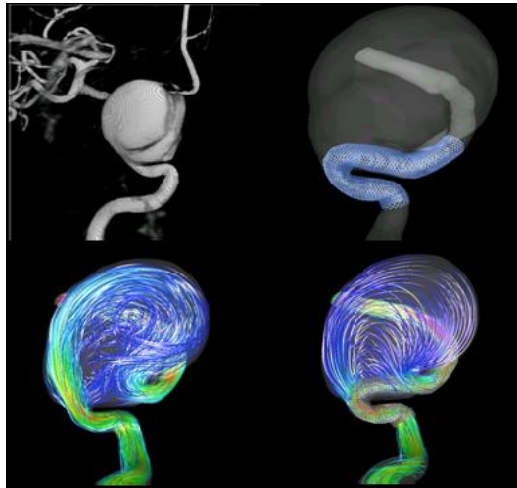


Figure 2.9: Patient-specific image based simulations of hemodynamics before and after aneurysm stenting.

Source : G.Canton, 2005

CHAPTER 3

METHODOLOGY

3.1 COMPUTATIONAL FLUID DYNAMICS

Computational fluid dynamics (CFD) is one of the branches of fluid mechanics that uses numerical methods and algorithm to solve and analyze problem that involve fluid flow. Computers are used to perform the millions of calculation required to stimulate the interaction of fluids and gases with the complex surfaces used in engineering.

The fundamental basis to CFD problem is the Navier-Stokes equations, which define any single-phase fluid flow. These equations can be simplified by removing terms describing viscosity to yield the Euler equation. Further simplification, by removing terms describing vorticity yields the full potential equations. Finally, these equations can be linearized to yield the linearized potential equations.

The most fundamental consideration in CFD is how one treats a continuous fluid in a discretized fashion on a computer. One method is to discretized the spatial domain into small cells to form a volume mesh or grid, and then apply the suitable algorithm to solve the equation of motion. If one chooses not to proceed with a mesh-based-method, a number of alternatives exist, notably are smooth-particle hydrodynamics (SPH), a Lagrangian method of solving fluid problem. Second is Spectral methods, a technique where are the

equations are projected onto basis functions like the spherical harmonics and Chebyshev polynomials. The most popular method is Lattice Boltzmann method (LBM), which simulates an equivalent mesoscopic system on a Cartesian grid, instead of solving the macroscopic system.

In all of these approaches the same basic procedure is followed. The process was divided into three parts which is pre-processing, solver and post-processing. This can be shown in Figure 3.1.

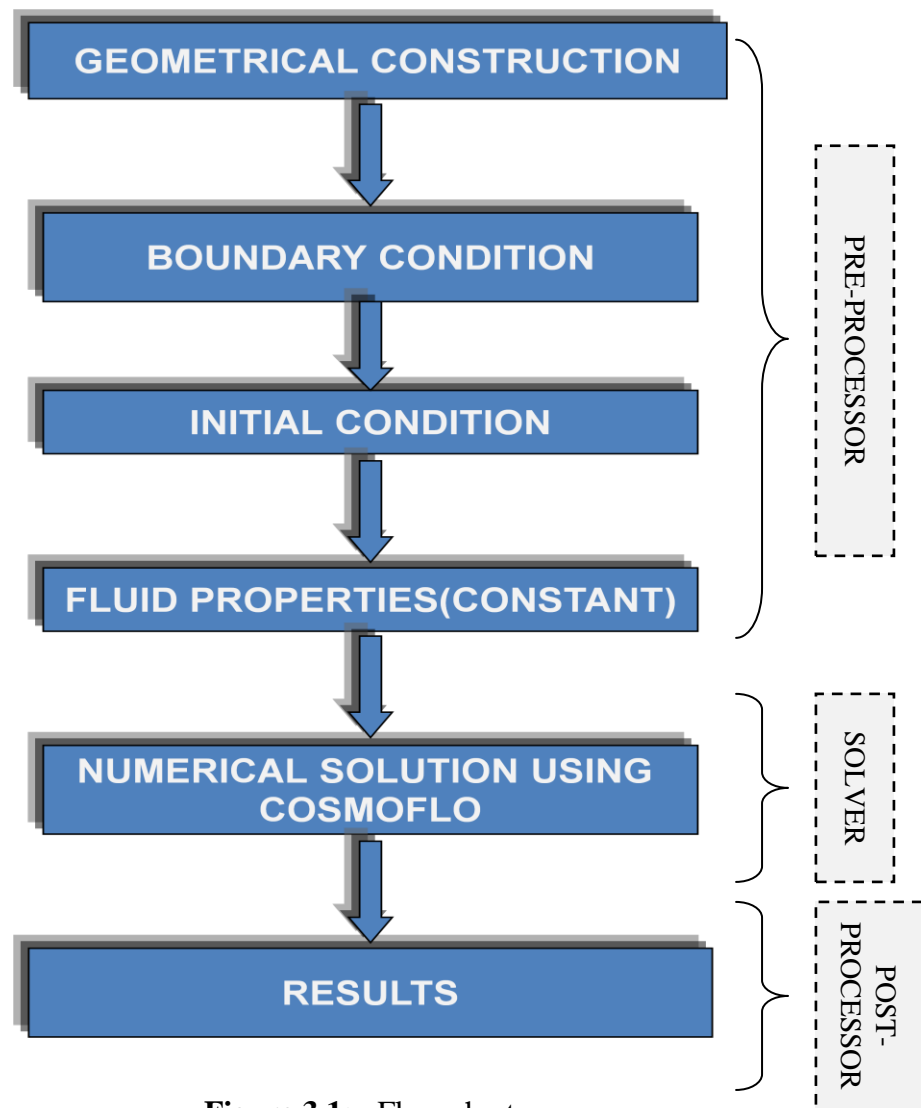


Figure 3.1: Flow chart

3.2 SIMULATION DETAILED

3.2.1 The Software

The SolidWork 2008 was applied to generate the geometries of the models and their computational meshes. The setup of the physical problem, the solution and the presentation and post processing of the results was performed by various modules of SolidWork 2008 which is CosmosFlow.

3.2.2 Geometry of the Model

The size and parameters of the simulations are chosen so as to correspond to the range of the experimental and clinical observations. The stent is a tubular mesh which fits perfectly with the parent vessel width. The stent is represented by horizontal struts with a thickness of two lattice cells. As for the aneurysm, it was 10 mm in diameter while the parent vessel is a straight tube, 8mm wide and 60 mm long.

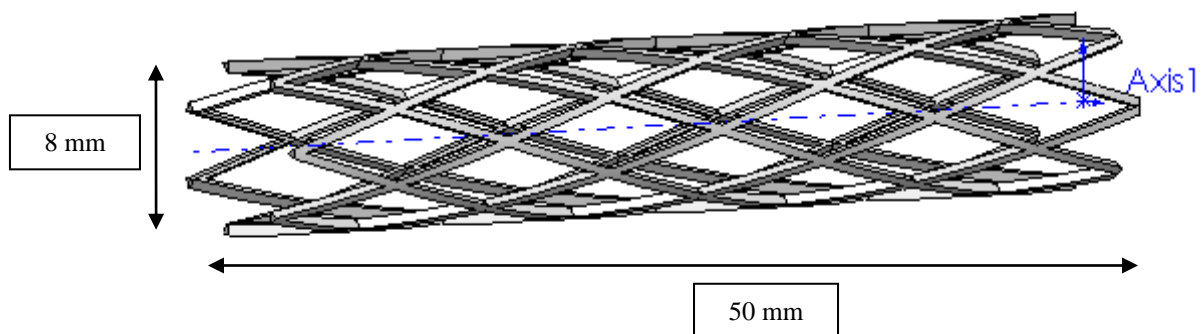


Figure 3.2: Geometry model of stent

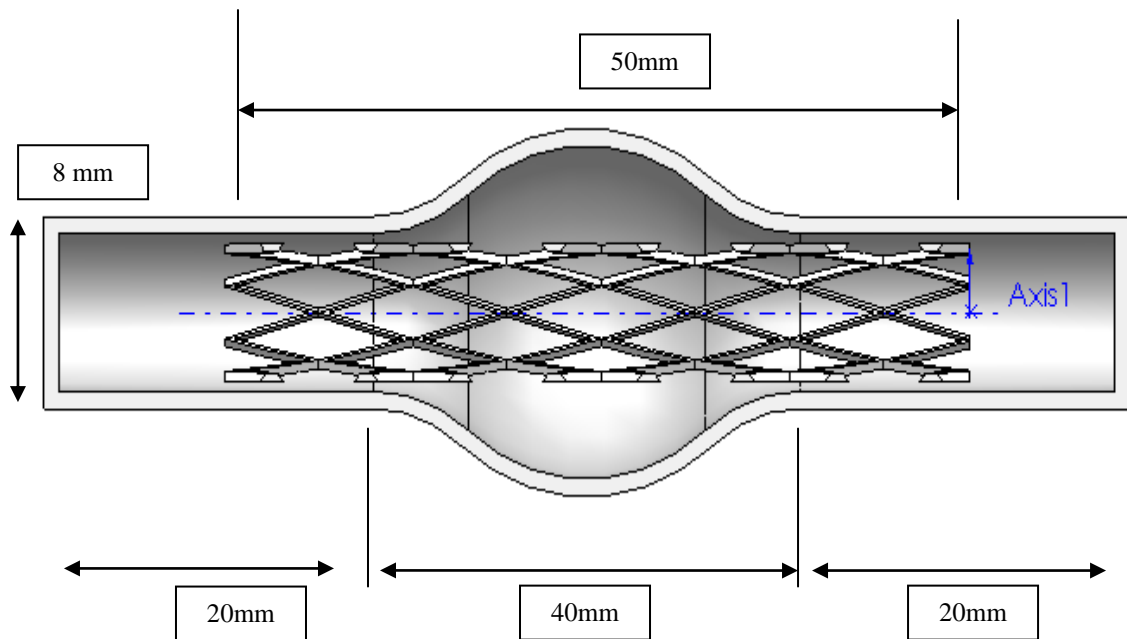


Figure 3.3: Geometry model of aneurysm with stent

Since this study is related to the effect of stent design to the blood flow, the stent design plays an important thing in order to get the correlation of stent strut angle and the behavior of the blood. To create the model of the stent, we have choose one design of the stent which is tube design. This design has applied to all stent but there have different strut angle. Five different strut angle have been choose for all stent which is 30° , 35° , 40° , 45° and 50° .

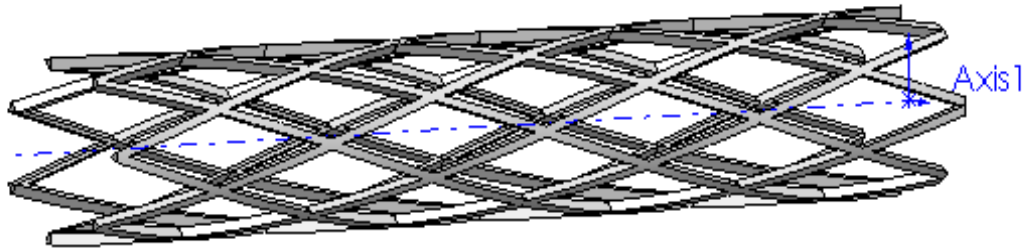


Figure 3.4: Stent with 30° of strut angle

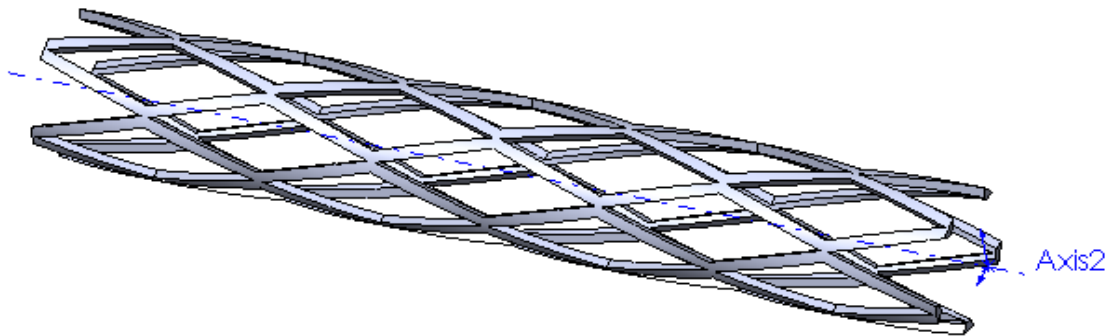


Figure 3.5: Stent with 35° of strut angle

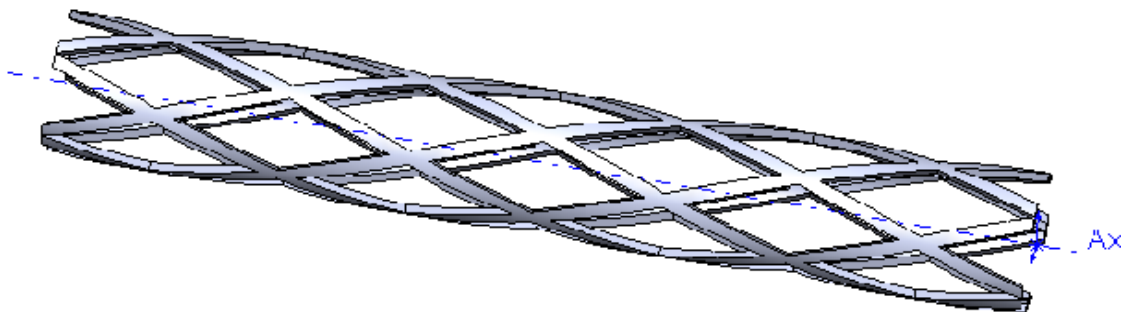


Figure 3.6: Stent with 40° of strut angle

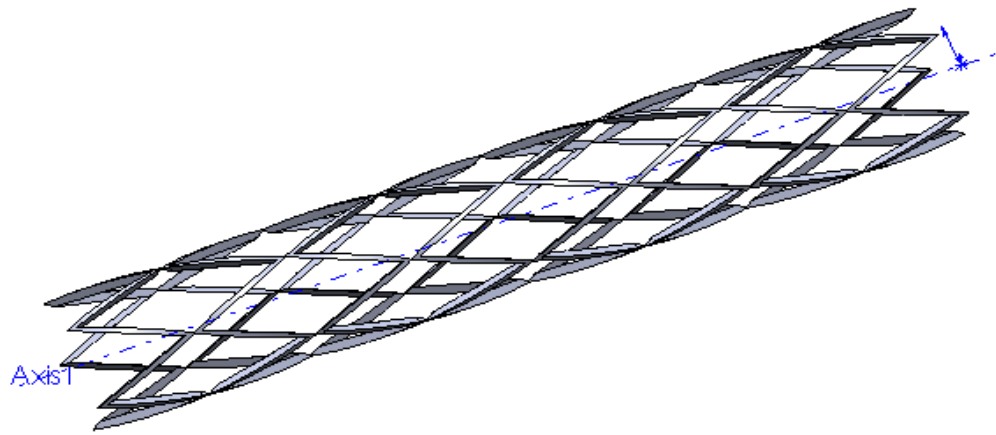


Figure 3.7: Stent with 45° of strut angle

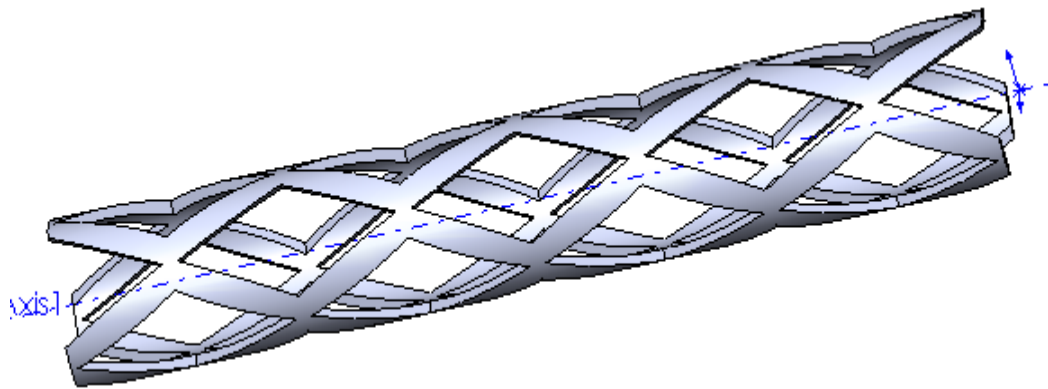


Figure 3.8: Stent with 50° of strut angle

3.2.4 Governing equation of blood flow

Blood flow in the artery is considered to be incompressible, consisting of the continuity and Navier-Stokes equations. The governing equations are return as follows for a computational domain Ω :

$$\frac{\partial u_i}{\partial x_i} = 0 \quad (1)$$

$$\begin{aligned} \rho \left(\frac{\partial u_i}{\partial t} + u_j \frac{\partial u_i}{\partial x_j} \right) &= - \frac{\partial P}{\partial x_j} + \mu \frac{\partial^2 u_i}{\partial x_j \partial x_j} \\ &+ f_i \end{aligned} \quad (2)$$

where

u_i = velocity in the i -th direction

P = pressure

f_i = body force

ρ = density

μ_i = viscosity

δ_{ij} = Kronocker delta

3.2.5 Assumptions parameter and boundary condition

For the simulations carried out in this study, it is assumed that the blood is an incompressible and Newtonian fluid. Blood behaves as non-Newtonian fluid since the viscosity decreases with increasing shear rate. This non-Newtonian effects becomes more significant in small diameter vessels ($<0.01\text{mm}$) and low shear rate ($<100 \text{ s}^{-1}$). In large vessels, the viscosity of blood is approximately 3.5cP. The Newtonian effect and non-Newtonian effect in aneurismal flow was compared and it was discovered that there was no significance difference in their results. Thus, the Newtonian blood property is assumed in this study. This assumption is reasonable since the diameter of the

internal carotid artery is about 0.5 cm on average and large enough compared to the size of a red cell, which is about 7.5 μm . The physical properties of blood in the simulations are set to be as $\rho = 1.00 \text{ g/cm}^3$. The blood flow can be assumed as laminar since the maximum Reynolds number is about 700. [21]

Boundary conditions were defined using specific parameters. Blood was assumed as an incompressible fluid with a specific gravity of 1053 kg/m^3 and a viscosity of $4.0 \times 10^{-3} \text{ N/m}^2$ per second. The viscoelastic properties of the vessel wall were neglected, and a rigid wall with no slip condition was assumed.[12]

3.2.6 Finite Volume Method

The finite volume method is a method of representing and evaluating partial differential equations as algebraic equations. Similar to finite difference method, values are calculated at discrete places on a meshed geometry. “Finite volume” refers to small volume surrounding each node point on a mesh. In the finite volume method, volume integrals in the partial differential equation that contain a divergence term are converted to surface integrals, using the divergence theorem. This term are then evaluated as fluxes at the surface of each finite volume. Because the flux entering a given volume is identical to that leaving the adjacent volume, these method are conservative. This finite volume is easily formulated to allow for unstructured meshes. This method is use as a solver in the simulation.

CHAPTER 4

RESULTS AND DISCUSSION

4.1 RESULTS

The changes of velocity and pressure in aneurysms were accessed by using computational fluid dynamic simulations with finite volume method as the solver. The placement of a stent in an artery affects the details of flow adjacent to the artery wall. The effect on overall flow pattern stem from structural aspects of the stent interaction. The degree to which these factors affect flow pattern depend strongly on stent design.

In this study, the effects of stent implementation to the aneurysm have been proven in reducing the pressure and increasing the minimum velocity in the stented aneurysm. The data analysis was compared for different value of stent strut angle to establish the correlation of stent strut angle to the behavior of blood flow.

4.2 VELOCITY PROFILE

The result for the velocity profile of all stents analyzed in this study is shown in Figure 4.1. From the graph, the minimum velocity obtained refers to the stent with 30° of strut angle which is the lowest angle used in this study. We observed that velocity reduced from 0.4 m/s to 0.3 m/s once it passes through the aneurysm sac. It means that when the blood flows into the aneurysm region, velocity reduction occurred. The vortex formation formed in the aneurysm region contributes to energy losses of the fluid and unable to recover after the flow entering back to the normal artery. In order to reduce

the flow activity, the stent design is an important thing that needs to be considered. In this study, we have choose to vary the stent strut angle to find the optimal performance of stent implementation.

According to previous study, the flow in an aneurysm is influenced to a large extent by the velocity profile in the upstream artery specifically for saccular aneurysm. They found that decreasing neck width reduces the amount of rotation in the aneurysm sac. However, when increasing the neck length similar results appeared but in addition the structure of the flow changes. Since the neck size for fusiform aneurysm is constant in this study, the effect of proximal neck sizing is proposed for further investigation in future study.

The strong dependence of flow stagnation on stent strut spacing was observed using a computational model. For a stent strut spacing of three strut heights, the wall shear stress between the struts was less than 18% of the smooth wall value. For a stent strut spacing of 12 strut heights, the flow reattached between the stent struts, and the wall shear stress was approximately 90% of the smooth wall value between the struts. They also included a simple model for arterial wall compliance, but the rigid wall results were not markedly affected. It is important to note that the strut shape did not affect the nature of the near-wall flow patterns. [29]

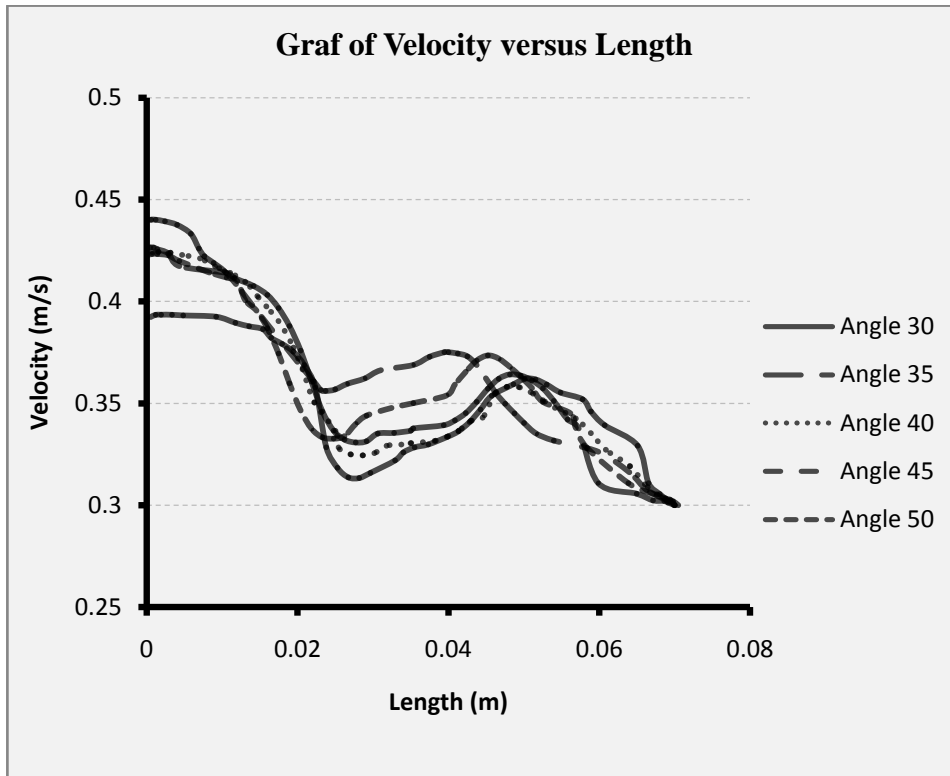


Figure 4.1: Velocity profile in aneurysm region

The large vortex formation that dominated in the aneurysm region has reduced when stent type IV is applied. The minimum velocity improvement for stent type IV is significant compared to stent type I, II and III. Stent type IV achieved 15% improvement of minimum velocity while stent type III achieved 7%. The minimum velocity improvement for stent type II is 5% compared to stent type I which is improved 4%. From the implementation of the stent, the minimum velocity can be increased which indicate that vortex formation in the aneurysm region will lead to the decreasing of velocity. The larger vortex formation gives the larger changes in velocity. Furthermore, different type of stents gives different results for velocity bandwidth. Velocity bandwidth is referred to the differences of minimum velocity obtained by the strut angle used to the minimum velocity obtained by the control model strut angle. The small values of velocity bandwidth indicate the velocity obtained is closely to the velocity of control model.

The data for minimum velocity for all types of strut angle used is simplified in Table 4.1. Figure 4.3 shows the velocity bandwidth for each type of stent used. For the conclusion, the stent with higher strut angle will gives better results which is can obtained the higher minimum velocity compared to other stent.

Table 4.1: Minimum velocity for all types of strut angle

NO	TYPE	STRUT ANGLE (°)	MIN. VELOCITY (m/s)
1		30	0.3137
2	I	35	0.3250
3	II	40	0.3308
4	III	45	0.3339
5	IV	50	0.3596

% of velocity:

Type I:

$$\% = \frac{0.3250 - 0.3137}{0.3137} \times 100\%$$

$$= 3.6 \%$$

Type II:

$$\% = \frac{0.3308 - 0.3137}{0.3137} \times 100\%$$

$$= 5.45 \%$$

Type III

$$\% = \frac{0.3339 - 0.3137}{0.3137} \times 100\%$$

$$= 6.44 \%$$

Type IV:

$$\% = \frac{0.3596 - 0.3137}{0.3137} \times 100\%$$

$$= 14.63 \%$$

Table 4.2: Percentage of minimum velocity for all types of stent strut angle

No	Type	Strut Angle (°)	Percentage (%)
1		30	0
2	I	35	3.6
3	II	40	5.45
4	III	45	6.44
5	IV	50	14.63

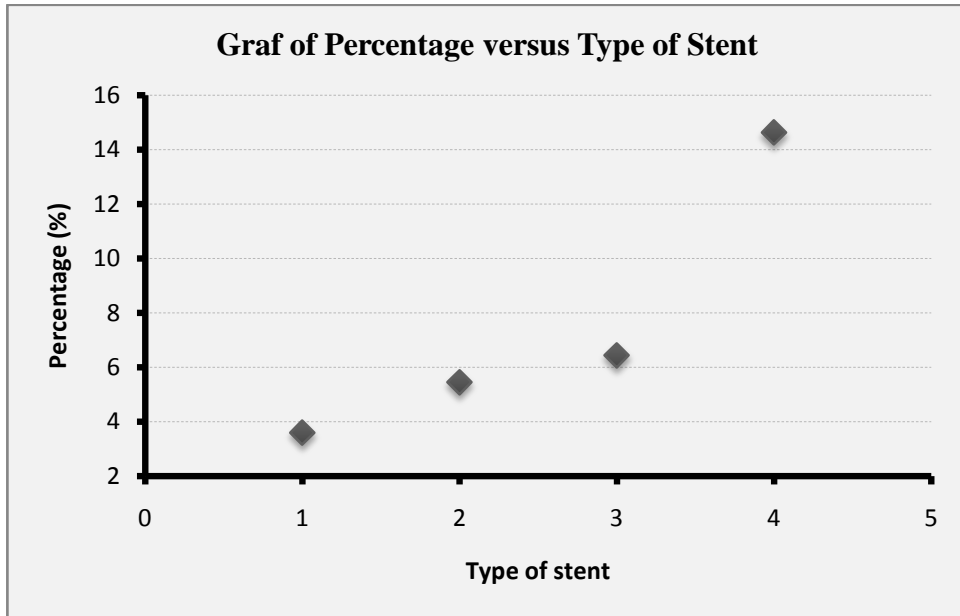


Figure 4.2: Percentage of velocity for 4 types of strut angle

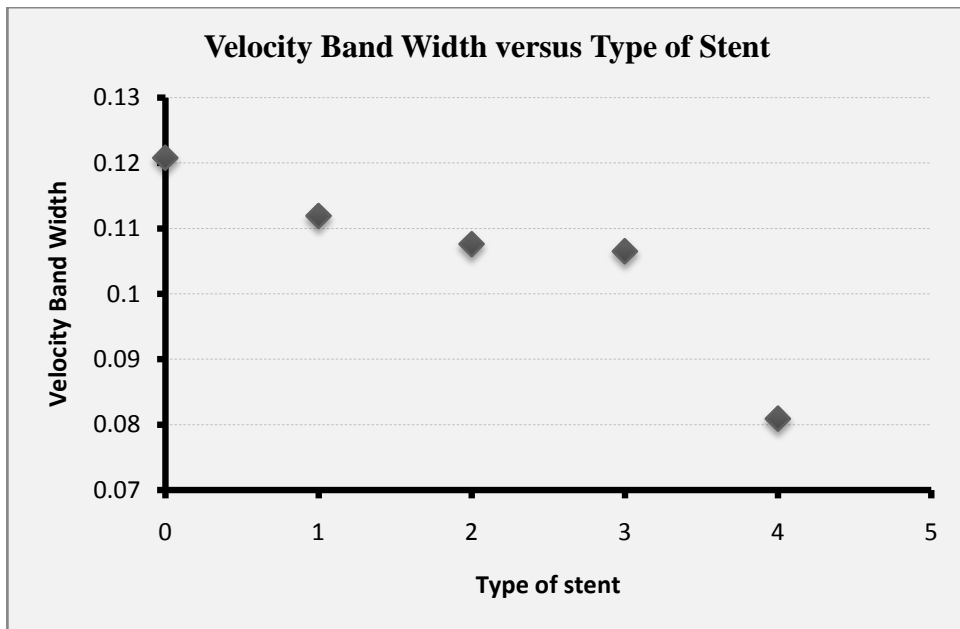


Figure 4.3: Velocity Bandwidth for each type of stent

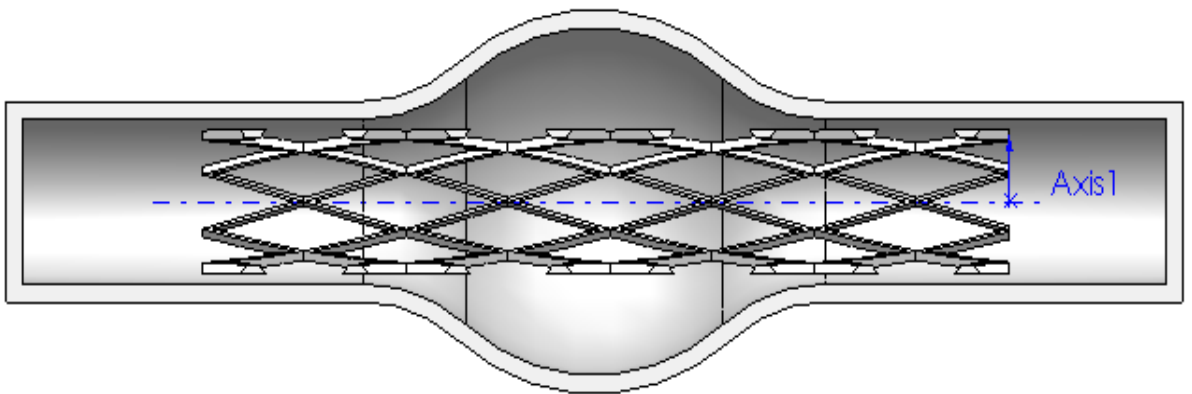


Figure 4.4: Stented Aneurysm Model

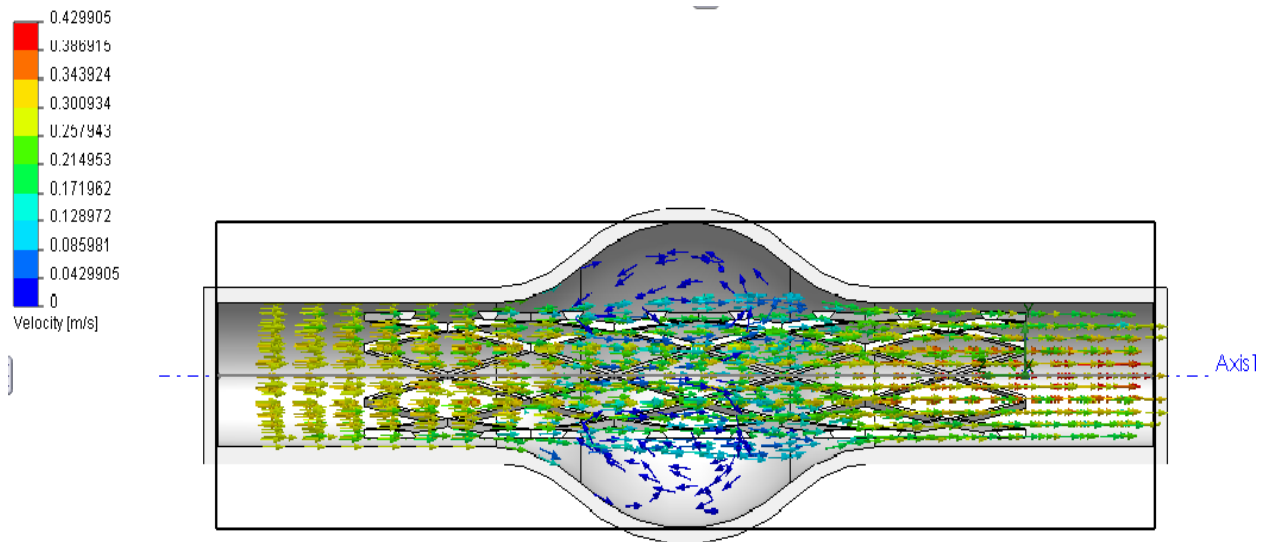


Figure 4.5: Stent with 30° strut angle velocity streamlines

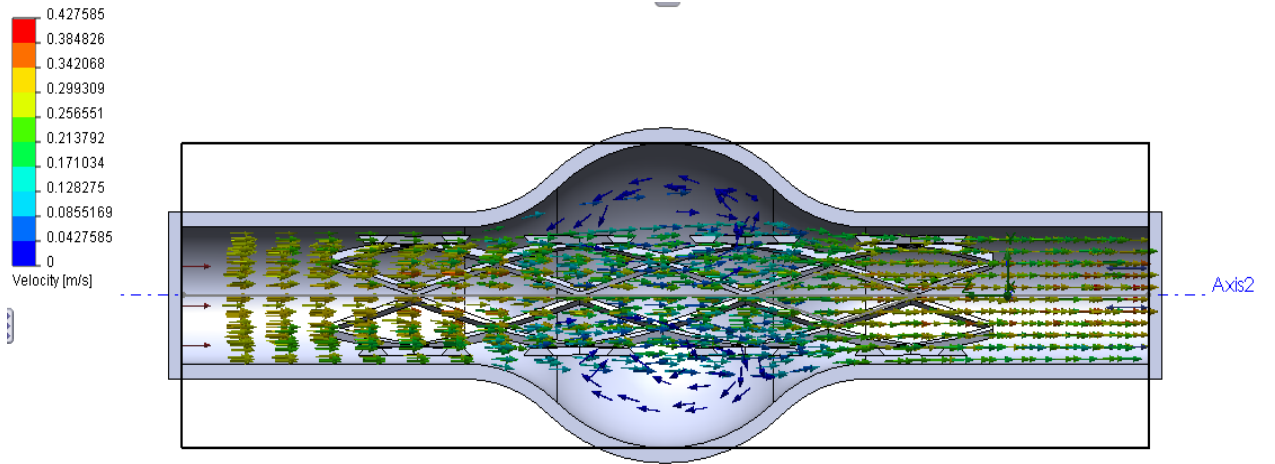


Figure 4.6: Stent with 35° strut angle velocity streamlines

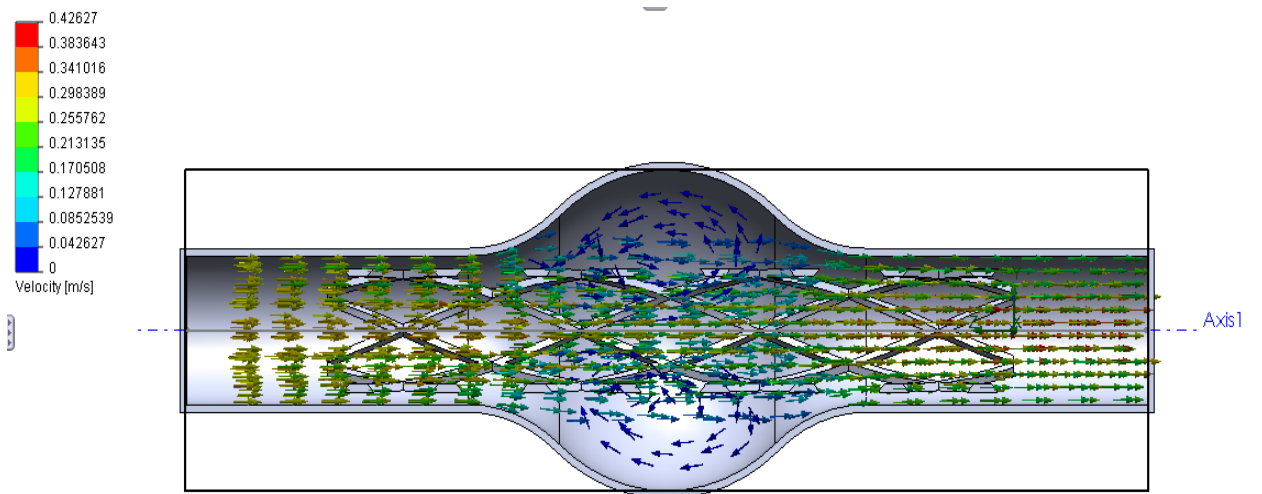


Figure 4.7: Stent with 40° strut angle velocity streamlines

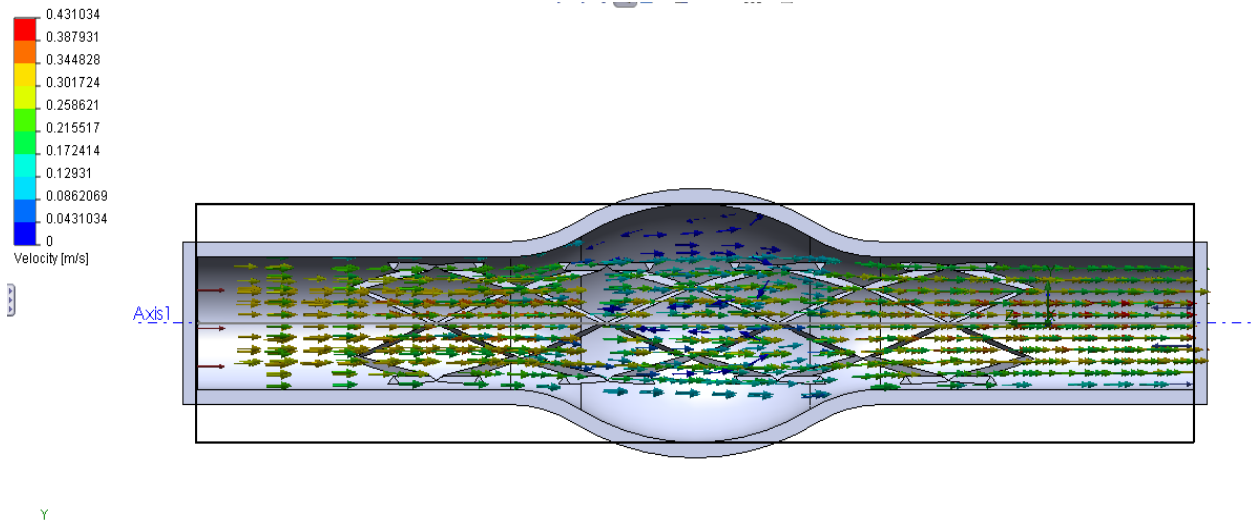


Figure 4.8: Stent with 45° strut angle velocity streamlines

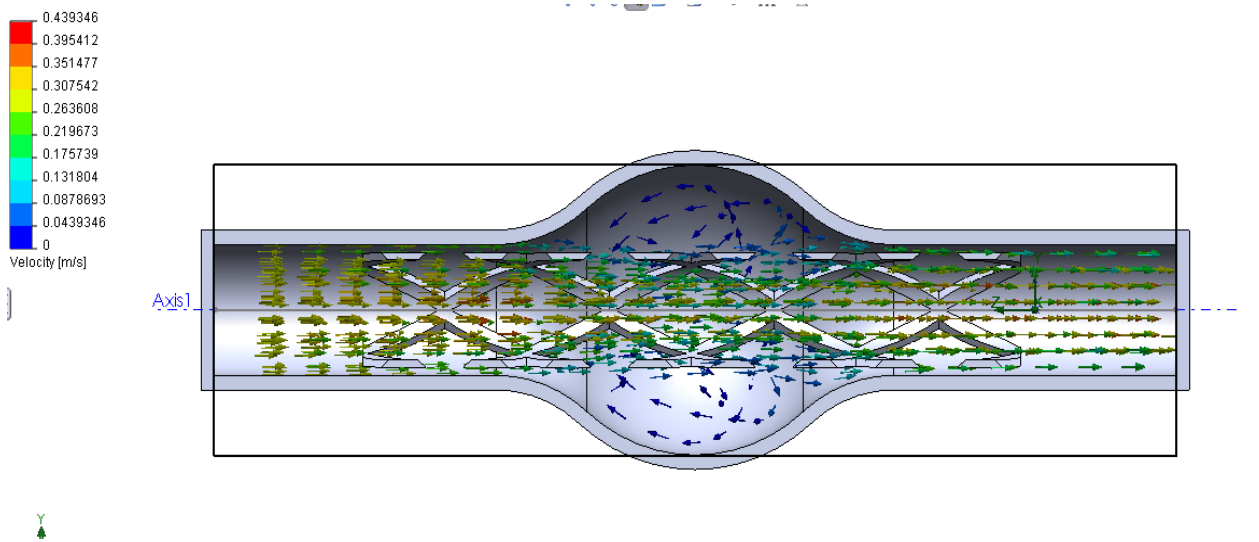


Figure 4.9: Stent with 50° strut angle velocity streamlines

4.3 PRESSURE

Pressure is another parameters considered in this study. In order to get the correlation between stent strut angle with the blood flow and to determine flow pattern in the blood, we need to investigate the pressure distribution in the aneurysm region. For the implementation of stents, the effect of stent strut disturb the blood flow in the aneurysm region causing the level of flow activity is higher but the pressure is reduced after the strut generate small scale of vortices as shown in Figure 4.12 to Figure 4.16.

The exit pressure should be higher than the inlet pressure due to the Bernoulli's principle that gives the relationship between velocity and pressure. Pressure magnitude for all type of stent used has follow this principles as shown in Figure 4.10. The detail for prove on the numerical calculation enclosed with sample calculation by substituting the results from simulation.

Table 4.4 shows the peak pressure obtained from all type of stent in order to determine the important parameters in pressure distribution in aneurysm dome. From the table, stent type I gives peak pressure of 496 Pa while stent type II gives 494 Pa of peak pressure. The implementation of stent type III gives peak pressure of 490 Pa and stent type IV for 501 Pa of peak pressure. Pressure distribution along the centerline of the aneurysm can be seen from Figure 4.10. These numerical results revealed some of the understanding towards predicting rupture of aneurysms where the local pressure at the distal end found to be the critical location.

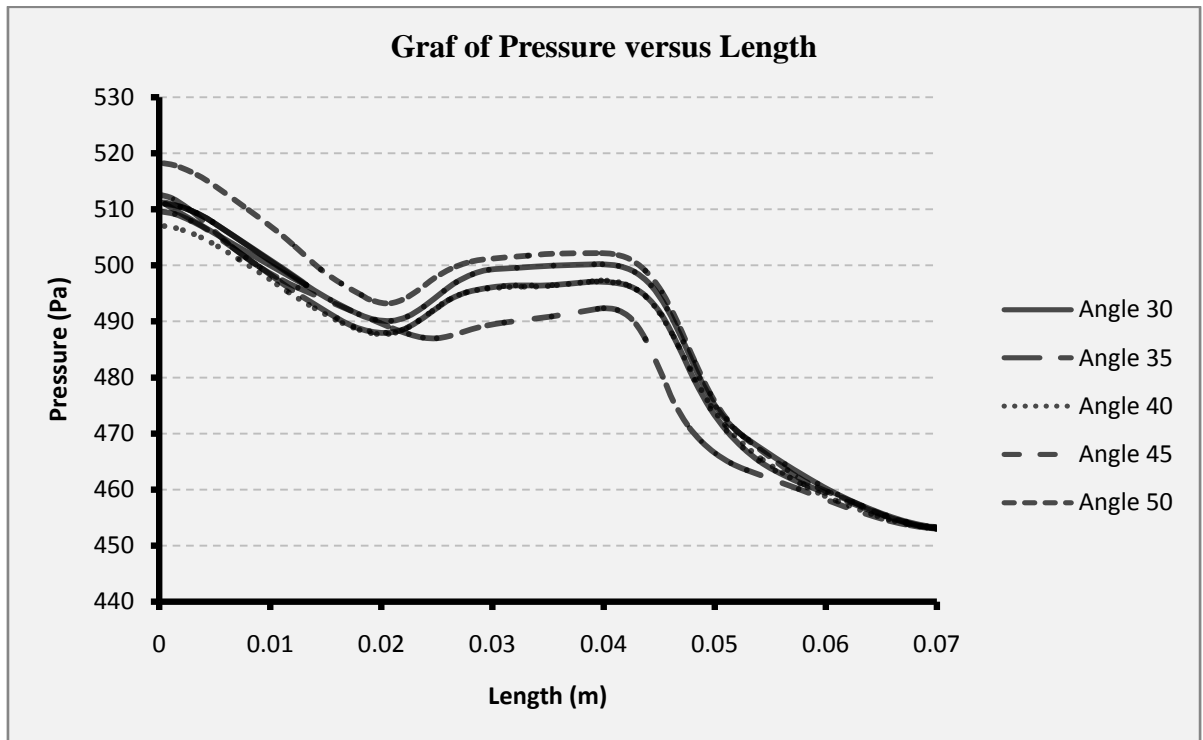


Figure 4.10: Pressure distribution for all stented aneurysm

From Figure 4.10, we can see the distribution of pressure plotted for all type of stent applied to the aneurysm. Pressure was decreasing when the blood flows through the artery but it suddenly increased once it has reached the aneurysm region. When the blood flows through aneurysm region, pressure was decreasing as before it enters the aneurysm region. In order to get pressure going decrease, the use of stent was applied to the aneurysm. With a different strut angle used for stent will gives a different performances of stent. The use of stent type IV gives the highest pressure while stent type III gives the lowest pressure. Besides, peak pressure for all type of stent used was obtained from the analysis as simplified in Table 4.3.

Equation of motion in Cartesian form is

$$\rho \left(\frac{\delta u_i}{\delta t} + u_j \frac{\delta u_i}{\delta x_j} \right) = -\frac{\delta p}{\delta x_i} + B_i \quad (4.1)$$

The component form for three dimensional

$$\rho \left(\frac{\delta u}{\delta t} + u \frac{\delta u}{\delta x} + v \frac{\delta u}{\delta t} + w \frac{\delta u}{\delta x} \right) = -\frac{\delta p}{\delta x} + B_x \quad (4.2)$$

$$\rho \left(\frac{\delta v}{\delta t} + u \frac{\delta v}{\delta x} + v \frac{\delta v}{\delta t} + w \frac{\delta v}{\delta x} \right) = -\frac{\delta p}{\delta y} + B_y \quad (4.3)$$

$$\rho \left(\frac{\delta w}{\delta t} + u \frac{\delta w}{\delta x} + v \frac{\delta w}{\delta t} + w \frac{\delta w}{\delta x} \right) = -\frac{\delta p}{\delta z} + B_z \quad (4.4)$$

These equations are also known as Euler equation for frictionless flow. Since, this study concern with the incompressible fluid, so the density is constant and the three equations plus continuity equation constitute four equations in four unknowns u, v, w and p . The convective terms make the solution becomes nonlinear

By rewriting in form of vector Euler equations

$$\frac{DV}{Dt} = \frac{\delta V}{\delta t} + (V \cdot \nabla)V = \rho \left[\frac{\delta V}{\delta t} + \nabla \left(\frac{V^2}{2} \right) - Vx(\Delta XV) \right] = -\nabla p + B \quad (4.5)$$

First integral of the equation of motion can be obtained by integrating the above equation between two points along the streamline. Let ds be an element blood particle of length along the streamline. Then

$$\rho \left[\frac{\delta V}{\delta t} \cdot ds + \nabla \left(\frac{V^2}{2} \right) \cdot ds - Vx(\Delta XV) \cdot ds \right] = -(\nabla p + \rho \nabla \phi) \cdot ds \quad (4.6)$$

Since V is parallel to ds , the term $Vx(\Delta XV)$ is perpendicular to ds and

$$Vx(\Delta XV) \cdot ds = 0 \quad (4.7)$$

Hence, for frictionless flow,

$$\int_1^2 \frac{\delta V}{\delta t} \cdot ds + \frac{V_2^2 - V_1^2}{2} + \int_1^2 \frac{\delta p}{\rho} + \varphi_2 - \varphi_1 \quad (4.8)$$

For steady state and gravitational potential is gz , then

$$\frac{V_2^2 - V_1^2}{2} + \int_1^2 \frac{p_2 - p_1}{\rho} + g(z_2 - z_1) = 0 \quad (4.9)$$

Therefore the generalized Bernoulli or Euler equation is

$$\frac{V_2^2 - V_1^2}{2} + \frac{p_2 - p_1}{\rho} + g(z_2 - z_1) = 0 \quad (4.10)$$

Since, this simulation is a blood vessel in the same arbitrary datum, the Bernoulli equation reduce to

$$\frac{V_2^2 - V_1^2}{2} + \frac{p_2 - p_1}{\rho} = 0 \quad (4.11)$$

Taking ($\rho=1$) as assumption for blood fluid, the pressure terms can be expressed as

$$p_2 - p_1 = \frac{V_1^2 - V_2^2}{2} \quad (4.12)$$

The exit pressure simply stated as

$$p_{exit} = \frac{V_1^2 - V_2^2}{2} + p_{inlet} \quad (4.13)$$

Here, it is proven that the exit pressure is always higher than the inlet pressure. For example, for predicting the exit pressure, we consider the aneurysm with 30° of strut angle.

Table 4.3: Data for two points in streamlines

Inlet (i)	Exit (e)
$P_{in} = 489$	P_{exit}
$X_1 = 0.0206$ m	$X_2 = 0.340$ m
$V_1 = 0.3904$ m/s	$V_2 = 0.340$ m/s

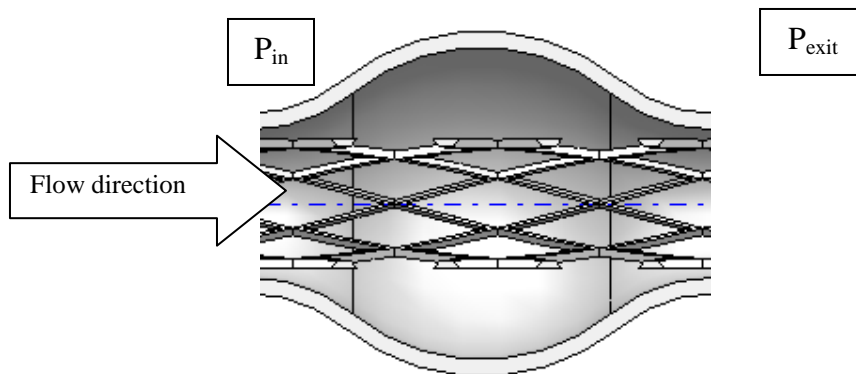


Figure 4.11: Flow direction in the aneurysm region

$$\begin{aligned}
 p_{exit} &= \frac{0.3904^2 - 0.340^2}{2} + 325 \\
 &= 489.02 \text{ Pa}
 \end{aligned}$$

The calculation shows that the exit pressure is higher than the inlet pressure as it follows Bernoulli's equation.

Table 4.4: Peak pressure for all type of strut angle

No	Type	Strut Angle (°)	Peak Pressure (Pa)
1		30	499
2	I	35	496
3	II	40	494
4	III	45	490
5	IV	50	501

From the analysis, we found that the highest peak pressure obtained by highest strut angle used to the stent. As the increasing of strut angle, peak pressure is decreasing but it was sudden change when stent type IV was applied which is the highest strut angle used. Peak pressure of the implementation of stent type IV had increased higher than other stent. It indicated that using too high of strut angle may increase peak pressure.

The correlation of peak pressure to the use of different stent strut angle in this project can be seen in Figure 4.12. In order to get the lowest peak pressure, the future study need to consider hemodynamic factors that may lead to the rupture of the aneurysm. The higher pressure will makes the weakening of wall artery that will lead to the rupture of aneurysm.

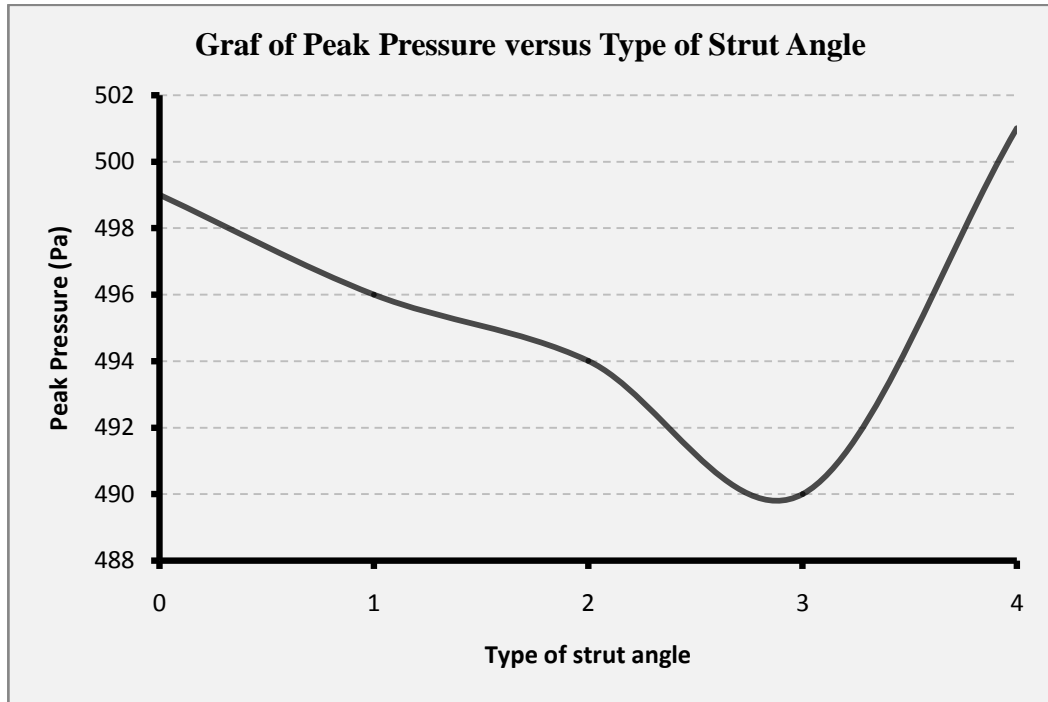


Figure 4.12: Correlation of peak pressure for all types of strut angle

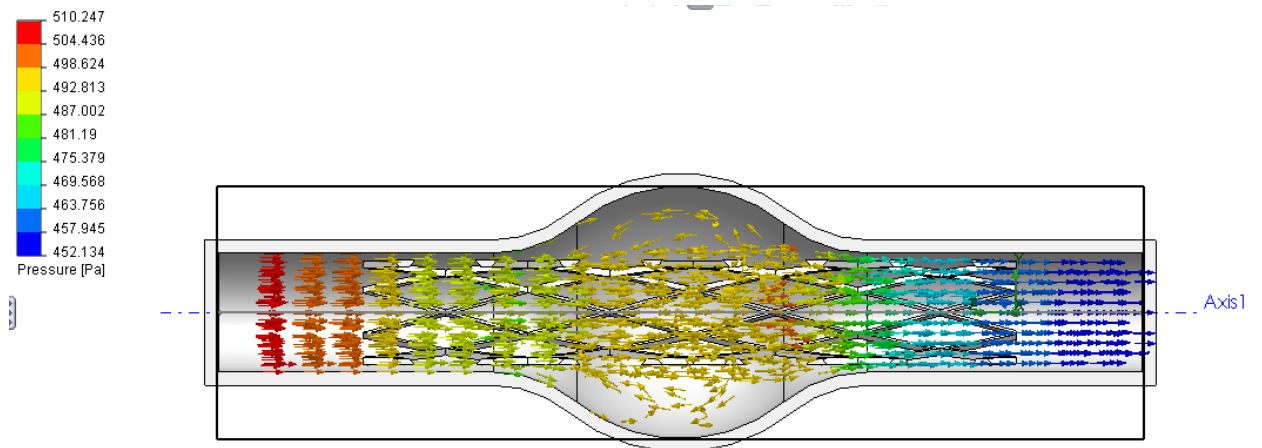


Figure 4.13: Stent with 30° strut angle pressure streamlines

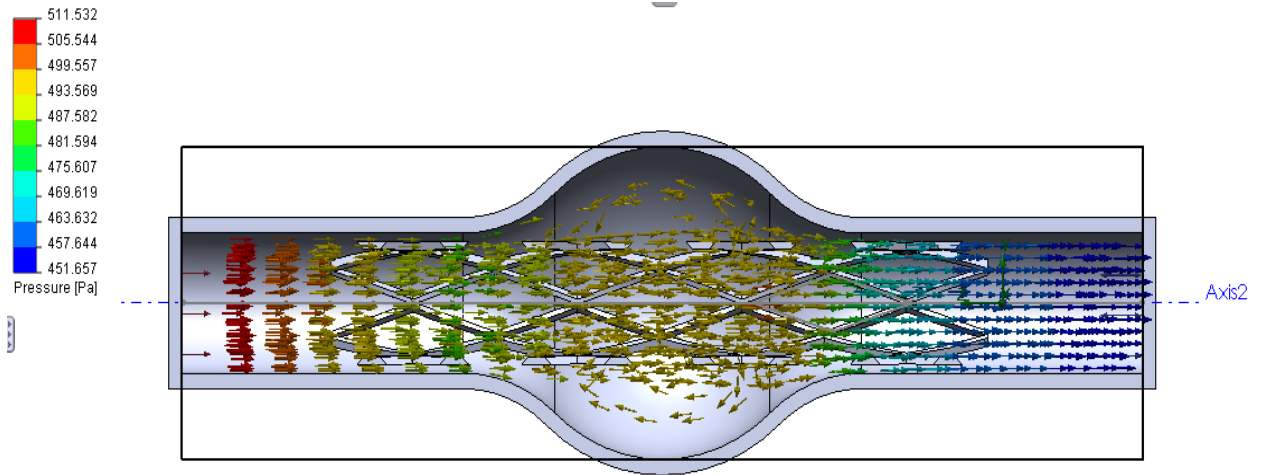


Figure 4.14: Stent with 35° strut angle pressure streamlines

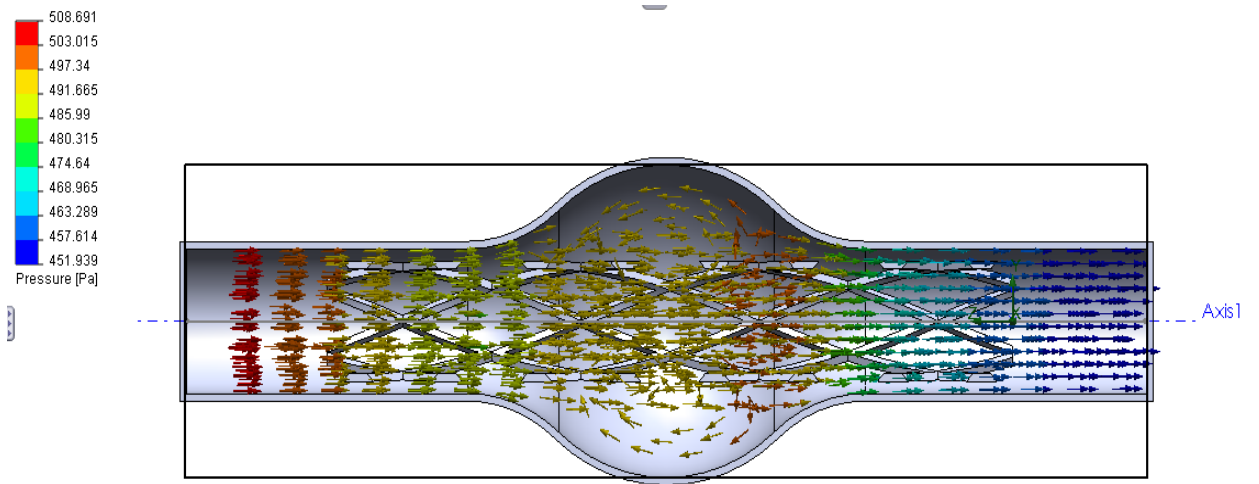


Figure 4.15: Stent with 40° strut angle pressure streamlines

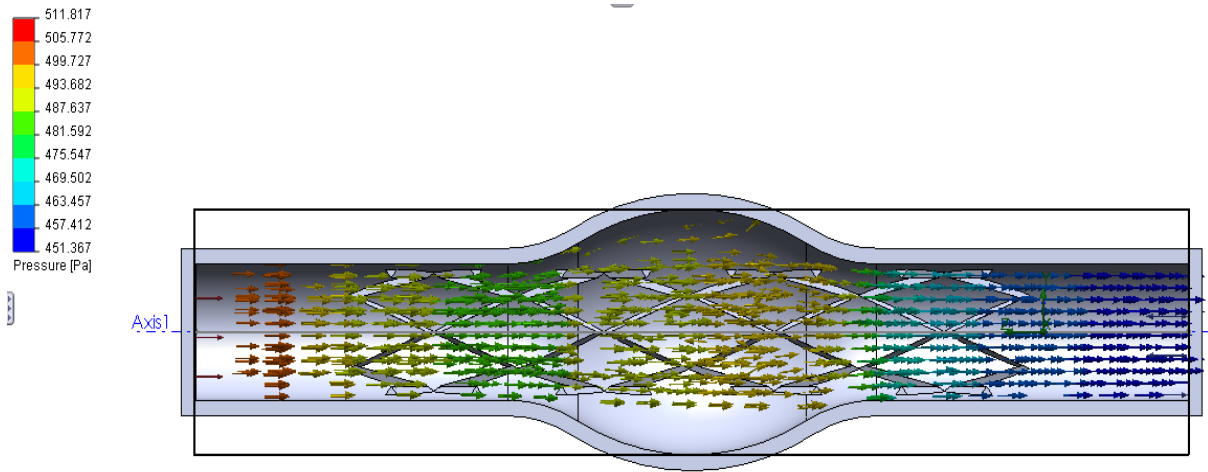


Figure 4.16: Stent with 45° strut angle pressure streamlines

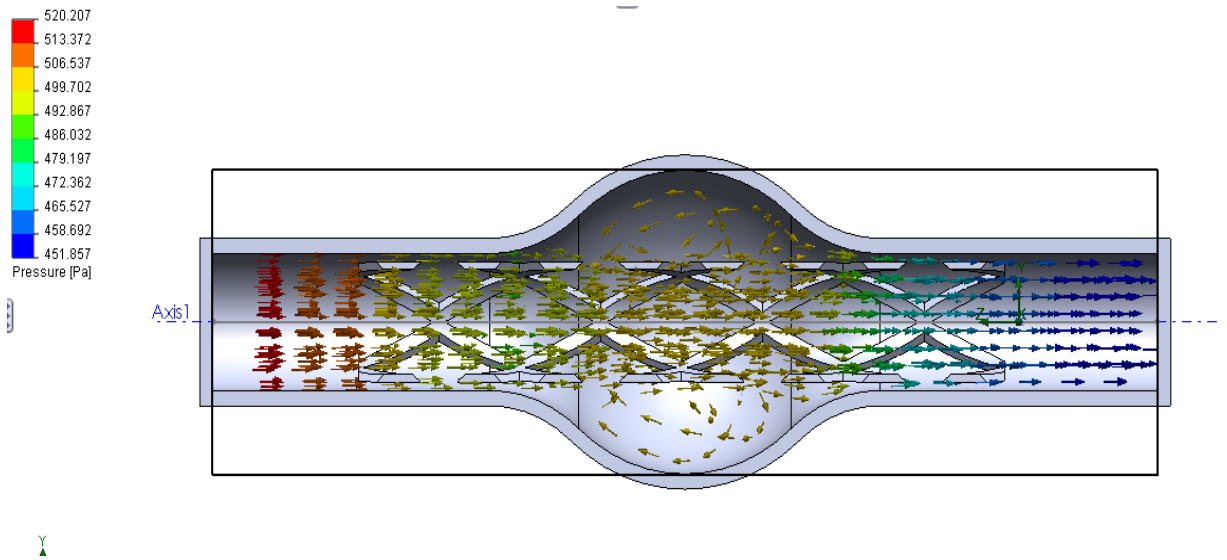


Figure 4.17: Stent with 50° strut angle pressure streamlines

CHAPTER 5

CONCLUSION AND RECOMMENDATION

5.1 CONCLUSION

This study establish the correlation between the stent strut angle and the velocity bandwidth. From the result obtained, the lowest peak pressure is 490 Pa with the use of 45° of strut angle. The highest peak pressure should results from the higher strut angle. However, stent with 50° of strut angle from type IV does not results the lowest peak pressure as expected.

The large vortex formation formed in the aneurysm sac has been reduced with the implementation of stent type IV. When stent type I is applied to the aneurysm, the minimum velocity increased by 3.6% while for the stent type II get increased by 5.45%. For stent type III, the minimum velocity increased by 6.44% but the most effective improvement of minimum velocity obtained by stent type IV which is increased 14.63%. Therefore, stent type IV gives the lowest velocity bandwidth compared to the other stent.

Finally, the effective stent should be satisfy the requirement of lowest velocity bandwidth and lowest peak pressure. However, too high a strut angle may cause higher peak pressure in the aneurysm region. Therefore, the stent angle has to be maintained within a certain range, which varies from 40° to 45°.

5.2 RECOMMENDATION

There are some recommendations should be made in order to get the better results for this study. Future studies should consider the recommendations to get the strong correlation of the variable or parameters used. The recommendations are:

1. Future study need to consider the interaction of blood flow characteristics such as pulsation. The pulsation may affect the behavior of the blood. It is also to analyze the blood-clotting ability in aneurysm by stent implementation to prevent the rupture.
2. The other variables that need to be considered is the interaction between the stent and the artery. The implementation of stent will gives an impact to the wall of the artery. This impact would affect the blood flow.
3. Design the stent that producing the preferable flow patterns in the aneurysm dome and reduce the positioning effect. Local flow pattern created by the stent should also be considered during stent design.

REFERENCES

- [1] M Kroon, G A Holzapfel, *A Theoretical model for fibroblast-controlled growth of saccular cerebral aneurysms*. Journal of Theoretical Biology
- [2] W P Park, S K Cho, Jai Y K, A Kristensson, S T S Al-Hassani, H S Kim, D Lim, *Evaluations of Stent performances using FEA considering a realistic balloon Expansion*. Proceedings of World Academy of Science, Engineering and Technology Volume 27 February 2008
- [3] Rossella Ballosino, Gervaso F, Migliavacca F, Gabriele Dubini, *Effect of different stent design on local hemodynamics in stented arteries*. Journal of Biomechanics 41(2008) 1053-1061
- [4] Gyorgy Paal, Adam Urgan, Istvan Szikora, Imre Bojtar, *Flow in simplified and real models of intracranial aneurysm*. International Journal of Heat and Fluid Flow 28 (2007) 653-664
- [5] Gador Canton, David I Levy, Juan C. Lasheras, Peter K. Nelson, *Flow changes caused by the sequential placement of stents across the neck of sidewall cerebral aneurysm*. J Neurosurg 103:891-902, 2005
- [6] M.Hirabayashi, M.Ohta, K Barath, Daniel A.R, B.Chopard, *Numerical analysis of the flow pattern in stented aneurysms and its relation to velocity reduction and stent efficiency*. Mathematics and Computers in Simulations 72 (2006) 128-133
- [7] M Oshima, R Torii, T Kobayashi, N. Taniguchi, K Tagaki, *Finite element simulation of blood flow in the cerebral artery*. Computer Methods in Applied Mechanics and Engineering 191 (2001) 661-671
- [8] C Rammohan, A Erdogan, C J Davidson, *New stent technologies: coated, covered and bifurcated stents*
- [9] Yi Qian, Tetsuji Harada, Koichi Fukui, Mitsuo Umezu, Hiroyuki Takao, Yuichi Miruyama, *Hemodynamics Analysis of Cerebral Aneurysm and Stenosed Carotid Bifurcation using Computational Fluid Dynamics Technique*.
- [10] Fernando Mut, Sunil Appanaboyina, Juan R.Cebral, *Simulation of stent deployment in patient-specific cerebral aneurysm models for their hemodynamics analysis*.2008
- [11] M Hirabayashi, M Ohta, Daniel A. R, B. Chopard, *A Lattice Boltzmann study of blood flow in stented aneurysm*. Future Generation Computer Systems 20 (2004) 925-934

- [12] Jou LD, Quick CM, Young WL, Lawton MT, Higashida R, Martin A, Saloner D. *Computational Approach to quantifying hemodynamics forces in giant cerebral aneurysm*. AJNR Am J Neuroradiol. 2003;24:1804-1810.
- [13] LaDisa Jr, JF. , Olson, LE. ,Guler, I. , Hettrick, DA. , Kersten, JR., Warltier, DC, Pagel, PS, 2005. *Circumferential vascular deformation after stent implantation alters wall shear stress evaluated with time dependent 3D computational fluid dynamics models*. Journal of Applied Physiology 98, 947-957.
- [14] Tominaga, R., Kambic, HE., Emoto, H., Harasaki, H., Sutton, C., Hollman, J., 1992. *Effects of design geometry of intravascular endoprotheses on stenosis rate in normal rabbits*. American Heart Journal 123, 21-28.
- [15] Rogers, C., Tseng, D.Y., Squire, J.C. & Edelman, E.R. (1999) *Balloon–artery interactions during stent placement. A finite element analysis approach to pressure, compliance, and stent design as contributors to vascular injury*, Circulation Research, vol. 84, pp. 378-383
- [16] Rogers, C., Edelman, ER., 1995. *Endovascular stent design dictates experimental restenosis and thrombosis*.Circulation 91, 2995-3001.
- [17] Ku ,DN., Giddens, DP., Zarins, CK., Glagov, S., 1985.*Pulsatile flow and atherosclerosis in the human carotid bifurcation*. Positive correlation between plaque location and low oscillating shear stress. Atherosclerosis. 5, 293-302.
- [18] Jin, S., Yang, Y., Oshinski, J., Tannembaum, A., Gruden., J., Giddens, D., 2004. *Flow pattern and wall shear stress distributions at atherosclerotic-prone sites in a human left coronary artery; an exploration using combined methods of CT and computational fluid dynamics*. Conference Proceeding: IEEE Engineering in Medicine and Biology Society 5, 3789-3791.
- [19] K.M. Khanafer et al., *Fluid–structure interaction of turbulent pulsatile flow within a flexible wall axisymmetric aortic aneurysm model*, European Journal of Mechanics B/Fluids (2008), doi:10.1016/j.euromechflu.2007.12.003
- [20] Katritsis, D., Kaiktsis, L., Chaniotis, A., Pantos, J., Efstathopoulos, EP., Marmarelis, V., 2007. *Wall shear stress: theretical considerations and method of measurement*. Progress in Cardiovascular Diseases 49, 307-329.
- [21] K. Perktold, R. Peter, M. Resch, *Pulsatile non-Newtonian blood flow simulation through a bifurcation with an aneurism*, Biorheology 26 (1989) 1011–1030.

- [22] Tateshima S., Vinuela F, Villablanca JP, Murayama Y, Morino T, Nomura K, et al. *Three-dimensional blood flow analysis in a wide-necked internal carotid-ophthalmic artery aneurysm*. J Neurosurg 99: 526-533, 2003
- [23] Egelhoff, C.J., Budwig, R.S., Elger, D.F., Khraishi, T.A., Johansen, K.H., 1999. *Model studies of the flow in abdominal aortic aneurysm during resting and exercise conditions*. Journal of Biomechanics 32, 1319-1329.
- [24] Gonzalez, G., Cho, Y.I., Ortega, H.V., Moret, J., 1992. *Intracranial aneurysm: flow analysis of their origin and progression*. American Journal of Neuroradiology 13, 181-188.
- [25] Liou, T, -M., Liao, C., -C., 1997. *Flowfield in lateral aneurysm models arising from parent vessel with different curvatures using PTV*. Experiments in Fluids 23, 288-298.
- [26] Liou, T, -M, Chang, W, -C, Liao, C, -C, 1997. *LDV measurements in lateral models aneurysm of various sizes*. Experiments in Fluid 23, 317-334.
- [27] Shipkowitz, T., Rodgers, V.G.J., Frazin, L.J., Chandran, K.B., 2000. *Numerical study on the effect of secondary flow in the human aorta on local shear stresses in abdominal aortic branches*. Journal of Biomechanics 33, 717-728.
- [28] Liou, T., -M., Liou, S., -N., Chu, K., L., 2004. *Intra-aneurysmal flow with helix and mesh stent placement across side-wall aneurysm pore of a straight parent vessel*. Journal of Biomechanical Engineering 126, 36-43.
- [29] Benard, N., Coisne, D., Donal, E., Perrault, R., 2003. *Experimental study of laminar blood flow through an artery treated by a stent implementation: characterization of intra-stent wall shear stress*. Journal of Biomechanics 36, 91-98.

APPENDIX A

DATA FOR PRESSURE OF BLOOD FLOW WITH STENT

(ANGLE 30°)

Length(m)	Pressure (Pa)
0.070504226	453
0.069804207	453.3329315
0.069108414	453.447299
0.067281515	454.2664198
0.065454952	455.4158171
0.063263077	457.1031806
0.061071202	459.1146833
0.05924464	461.0411143
0.05632214	464.5490126
0.053034327	468.8899962
0.051573077	471.2368251
0.050111827	474.7312761
0.048650577	479.9063472
0.047189327	486.3305334
0.045728077	492.2325986
0.044266827	496.3807979
0.042805577	498.7861582
0.041344327	499.8821651
0.039883077	500.1912929
0.039152452	500.1843028
0.035499327	499.9133657
0.032211515	499.5687999
0.029654327	499.1955872
0.028193077	498.4185917
0.026731827	496.9799561
0.02563589	495.4471651
0.023809327	492.6398751
0.022348077	490.8586518
0.020886827	490.0795719
0.019425577	490.2890595
0.017964327	491.2695985
0.01540714	493.8317295
0.013215265	496.4489997
0.004813077	507.7211405
0.003351827	509.3053731
0.001890914	510.4638408
0.000495775	510.9755434
0.013215265	496.4489997
0.004813077	507.7211405
0.003351827	509.3053731
0.001890914	510.4638408
0.000495775	510.9755434

DATA FOR PRESSURE OF BLOOD FLOW WITH STENT
(ANGLE 35°)

Length (m)	Pressure (Pa)
0.07	453
0.069536138	453.2548731
0.068608414	453.4863204
0.067146827	454.1321332
0.065320265	455.3044559
0.058014015	460.960123
0.055456827	463.3599831
0.053995577	465.0955191
0.052534327	467.4313274
0.051073077	470.4664486
0.049611827	474.4126005
0.048150577	479.5726738
0.046689327	485.7370087
0.045228077	491.1338569
0.043766827	494.5481031
0.042305577	496.2733816
0.040844327	496.9178942
0.039383077	497.0905001
0.038652452	497.0169285
0.035365144	496.4505894
0.033538077	496.3857244
0.032076827	496.3885004
0.03098089	496.2683364
0.02951964	495.9382334
0.027693077	495.1944083
0.026231827	494.0266161
0.02513589	492.5979513
0.023309327	489.9785968
0.021848077	488.4809366
0.020386827	487.9660744
0.018925577	488.2177518
0.017464327	489.1118162
0.016003077	490.5615101
0.01198464	495.5545302
0.008696827	500.1851531
0.004313077	506.3116842
0.002851827	507.9332717
0.001390914	509.1132727
0	509.6363567

DATA FOR PRESSURE OF BLOOD FLOW WITH STENT
(ANGLE 40°)

Length (m)	Pressure (Pa)
0.069916768	453.0308569
0.069436359	453.2093457
0.068475542	453.3888137
0.067279699	453.8480707
0.065685516	454.6490355
0.064091425	455.6570791
0.060903243	458.0157954
0.059309152	459.4043778
0.057715062	461.0684107
0.056120971	462.9467681
0.054128357	465.5734468
0.052534266	468.170217
0.050940175	471.4831597
0.049346084	475.9049555
0.047751993	481.6349848
0.046157902	487.8250128
0.044563812	492.771846
0.042969721	495.6560459
0.04137563	496.9765092
0.039781539	497.296516
0.038984493	497.171631
0.034999266	496.3030326
0.03260813	496.1864067
0.030615516	496.0221043
0.028622902	495.5735129
0.027028812	494.7519193
0.025434721	493.0900285
0.024239152	491.3621677
0.022246539	488.7341402
0.020652448	487.7465813
0.019058357	487.8859039
0.017464266	488.8367576
0.015870175	490.2667911
0.013479039	492.920157
0.011486425	495.352245
0.009892334	497.5193125
0.007102675	501.1500144
0.004711539	503.9981378
0.003117448	505.5104607
0.001523724	506.6233275
0	507.1077721

DATA FOR PRESSURE OF BLOOD FLOW WITH STENT
(ANGLE 45°)

Length (m)	Pressure (Pa)
0.07	453
0.069112909	453.1977293
0.067206566	453.7354198
0.065059423	454.7774642
0.061838709	456.8551475
0.057544423	460.0949002
0.05289228	463.4507272
0.051460852	464.7015263
0.050029423	466.4730089
0.048776923	468.6462044
0.047524423	471.5389979
0.046271923	475.8127339
0.045332548	480.0541815
0.043766923	486.8611093
0.042514423	490.4183086
0.041261923	492.0273196
0.040009423	492.3377147
0.039472638	492.2050091
0.035312981	490.8744984
0.031062995	489.7839412
0.028736923	488.9292278
0.026231923	487.4555013
0.024979423	486.978417
0.023726923	487.1079999
0.022474423	487.7142122
0.020595673	489.0759239
0.012454423	496.0235775
0.010575673	497.894904
0.00905478	499.6742189
0.00780228	501.3840597
0.006191923	503.8982707
0.003865852	508.0741538
0.002613352	510.1260345
0.001182212	511.9486301
0	512.642125

DATA FOR PRESSURE OF BLOOD FLOW WITH STENT
(ANGLE 50°)

Length (m)	Pressure (Pa)
0.07	453
0.069652103	453.1644597
0.068608414	453.4458941
0.067512224	453.9529573
0.065320265	455.3428263
0.062397765	457.8061588
0.06020589	459.5899925
0.058379327	461.173232
0.05728339	462.4728957
0.056552765	463.4373807
0.052534327	469.5097929
0.051073077	472.5807538
0.049611827	477.1076046
0.048150577	483.0660149
0.046689327	489.6727965
0.045228077	495.2918286
0.043766827	499.0196381
0.042305577	501.1176594
0.040844327	501.9857546
0.039383077	502.1393809
0.035365144	502.0256012
0.033172765	501.7290863
0.029154327	501.0388033
0.027693077	500.4772611
0.026231827	499.3740334
0.024770577	497.6941604
0.023309327	495.5590326
0.021848077	493.812068
0.020386827	493.1901918
0.018925577	493.9155784
0.018194952	494.6801641
0.01636839	496.7531818
0.014541827	499.24266
0.01198464	503.759559
0.01052339	506.1740756
0.00760089	510.5273529
0.004313077	515.0554322
0.002851827	516.6531059
0.001390914	517.8189575
0	518.3347326

APPENDIX B

DATA FOR VELOCITY OF BLOOD FLOW WITH STENT

(ANGLE 30°)

Length (m)	Velocity (m/s)
0.070504226	0.392469706
0.069804207	0.393528613
0.069108414	0.393556523
0.068012224	0.393550255
0.06655089	0.393256993
0.06508964	0.392570884
0.06070589	0.389566496
0.058879327	0.387914458
0.05778339	0.386491438
0.05486089	0.382254625
0.053034327	0.379203123
0.051573077	0.375453027
0.050111827	0.368797811
0.048650577	0.357848019
0.045728077	0.328431149
0.044266827	0.318358513
0.042805577	0.313754837
0.041344327	0.3134315
0.039883077	0.315941519
0.03732589	0.32197736
0.035499327	0.325899309
0.034038077	0.328412894
0.03294214	0.329883719
0.029654327	0.333661361
0.028193077	0.336366654
0.026731827	0.340816967
0.025270577	0.346937769
0.023809327	0.353775156
0.022348077	0.35938598
0.020886827	0.362121482
0.019425577	0.361775164
0.017964327	0.359203209
0.016503077	0.355339443
0.01540714	0.352000464
0.013580577	0.346038562
0.011754015	0.339294274
0.009196827	0.32924612
0.004813077	0.310795043
0.003351827	0.305537456
0.001890914	0.302367658
0.001195458	0.301946512
0.000495775	0.3

DATA FOR VELOCITY OF BLOOD FLOW WITH STENT
(ANGLE 35°)

Length (m)	Velocity (m/s)
0.07	0.426369587
0.069072276	0.426543784
0.068608414	0.426468155
0.067146827	0.425686998
0.064954952	0.423635605
0.059840577	0.417403577
0.05728339	0.414017736
0.05582214	0.411510838
0.053995577	0.407602181
0.052534327	0.403174377
0.051073077	0.396814059
0.049611827	0.387951087
0.048150577	0.375852159
0.046689327	0.360654554
0.045228077	0.346110497
0.043766827	0.336672646
0.042305577	0.33218025
0.040844327	0.330806432
0.039383077	0.331370508
0.035365144	0.335200621
0.035	0.335525377
0.032807452	0.336550486
0.030615577	0.337724143
0.029154327	0.339291384
0.027693077	0.341629102
0.026231827	0.345237082
0.024770577	0.350715172
0.023309327	0.357133995
0.021848077	0.362140803
0.020386827	0.364223985
0.018925577	0.363665083
0.017464327	0.361290399
0.016003077	0.35740011
0.014176515	0.351261535
0.011619327	0.342189104
0.01052339	0.337695686
0.004313077	0.311025146
0.002851827	0.305647314
0.001390914	0.302412915
0.000927276	0.302128551
0.000463639	0.301379202
0	0.3

DATA FOR VELOCITY OF BLOOD FLOW WITH STENT
(ANGLE 40°)

Length (m)	Velocity (m/s)
0.069916768	0.424036824
0.069436359	0.424360431
0.068955951	0.424424073
0.067678313	0.423971443
0.066084039	0.422961422
0.064091425	0.421118649
0.060903243	0.417233484
0.05891063	0.414088963
0.056918016	0.409720113
0.054128357	0.402691446
0.052534266	0.397552598
0.050940175	0.390398976
0.049346084	0.380421638
0.047751993	0.366675083
0.046157902	0.350456168
0.044563812	0.336547285
0.042969721	0.32835909
0.04137563	0.32503121
0.039781539	0.324508305
0.038187448	0.325662767
0.034999266	0.329237717
0.033793477	0.329874579
0.031811084	0.330521379
0.030216993	0.331602041
0.028622902	0.333619582
0.027028812	0.336616773
0.025434721	0.341436974
0.025036198	0.343133262
0.022246539	0.354735586
0.020652448	0.35812824
0.019058357	0.357962403
0.017464266	0.355451025
0.015870175	0.351489053
0.014674607	0.347831646
0.013080516	0.342589983
0.011087902	0.335417211
0.009095289	0.327264335
0.007102675	0.319254687
0.004711539	0.310281891
0.003117448	0.305281565
0.001523724	0.3022416
0.000761862	0.30182838
0	0.300000002

DATA FOR VELOCITY OF BLOOD FLOW WITH STENT
(ANGLE 45°)

Length (m)	Velocity(m/s)
0.07	0.439943291
0.069408606	0.440234314
0.068817212	0.44020308
0.066311923	0.439426367
0.063985852	0.437634343
0.059870495	0.433227517
0.053965852	0.42598641
0.05163978	0.422289993
0.050029423	0.418966671
0.048776923	0.415036305
0.047524423	0.408593314
0.046271923	0.39823476
0.043766923	0.370453761
0.042514423	0.360816611
0.041261923	0.356542986
0.040009423	0.356158905
0.039472638	0.356821456
0.037504423	0.359620012
0.035312981	0.362301324
0.031062995	0.366341862
0.028915852	0.368898491
0.026545048	0.372936301
0.024979423	0.375142269
0.023726923	0.375160839
0.023100673	0.374422739
0.022161298	0.373117459
0.019969423	0.368843269
0.014020048	0.355255301
0.011828173	0.349752053
0.010262548	0.345165889
0.008875852	0.340347004
0.007623352	0.33516558
0.006907638	0.331775877
0.005834066	0.326303601
0.00404478	0.316225967
0.002434423	0.307474826
0.001182212	0.303263648
0.000591107	0.302700008
0	0.3

DATA FOR VELOCITY OF BLOOD FLOW WITH STENT
(ANGLE 50°)

Length (m)	Velocity (m/s)
0.07	0.422691207
0.069304207	0.423401948
0.06895631	0.423361128
0.067146827	0.422660748
0.063859015	0.419911117
0.058379327	0.414310436
0.056918077	0.411841465
0.056187452	0.410062717
0.052534327	0.400618757
0.051073077	0.39556955
0.049611827	0.386903357
0.048150577	0.374423075
0.046689327	0.359872537
0.045228077	0.346578798
0.043766827	0.337629708
0.042305577	0.333300422
0.040844327	0.332668273
0.03974839	0.333922736
0.035365144	0.339903747
0.03244214	0.344074615
0.029154327	0.347753976
0.027693077	0.350216185
0.026231827	0.3539843
0.024770577	0.359210412
0.023309327	0.365515781
0.021848077	0.371006829
0.020386827	0.373508749
0.018925577	0.371980459
0.017464327	0.367852325
0.016003077	0.3630572
0.014541827	0.357593294
0.013080577	0.350758568
0.01198464	0.345096142
0.01052339	0.337953372
0.008331515	0.328158667
0.004313077	0.310872392
0.002851827	0.305573574
0.001390914	0.302381716
0.000695457	0.301959102
0	0.300000004